

بسم الله الرحمن الرحيم

UNIVERSITY OF KHARTOUM

**FACULTY OF ENGINEERING &
ARCHITECTURE**

DEPARTMENT OF CHEMICAL ENGINEERING

**STUDY OF HYDRODYNAMICS AND MASS TRANSFER OF OIL
EMULSION IN A PILOT SCALE SIEVE TRAY COLUMN**

*A Thesis Submitted in Fulfillment Of the Requirements
For the Degree Of Ph.D in Chemical Engineering*

Presented By

Osman Tageldin Osman

Supervised By

Dr. Gurashi Abdalla Gasmelseed

Late : Dr. Osama Abdelhameed Abdalla

August 2005

Dedication

To the soul of great father

To my mother, wife and sons

With love

Acknowledgements

I would like to express my thanks to my late supervisor *Dr.Osama.Abdelhameed Abdalla* for his unlimited help, guidance, constant indispensable encouragement and invaluable comments during the preparation of this thesis.

Also I would like to express my gratitude to *Dr.Gurashi Abdalla Gasmelseed* for supervision and help in this thesis.

My thanks are also due to the staff of the chemical engineering department and the Unit Operation Laboratory staff in the University of Khartoum.

Abstract

A study of primary and secondary treated liquid petroleum wastes in a pilot sieve tray column has been undertaken. The literature related to this type of extractor and the relevant phenomena of droplet break-up and coalescence, drop size and drop mass transfer have been reviewed.

The method of treatment in local refineries has been investigated and it is observed that the primary and secondary processes are quite efficient, but the tertiary process leaves some of the oil in the effluent and this is why the treated water is not recycled and reused. The treated waste/oil water is pumped into ponds for evaporation leaving the oil and other less volatile components as a residue which have a negative impact on the environment.

The system of oil in water is not a normal solute-solvent system, and to make it so the mixture has been emulsified with a surfactant producing a partially water miscible emulsion. Experiments were carried out with non-mass transfer to determine the operating column hydrodynamics such as flooding. At 85% of flooding, mass transfer experiments were performed and the effects of drop size, drop size distribution and dispersed phase holdup volume at variable agitation speeds on the column performance have been investigated.

The concentration profile has been measured and the overall experimental mass transfer coefficients were calculated from the mean driving force using Simpson's rule. It is observed that drop size, drop size distribution and mass transfer coefficients were strongly dependent on the speed of agitation. As the oil droplets were composed of emulsified oil in water and the oil itself is completely immiscible in water, the direction of mass transfer was from the emulsified droplets to the dispersed phase. This condition coupled with high solubility of oil in n-hexane made the extraction process very efficient and an almost oil-free water could be obtained and recycled.

This work is also mainly intended to compare the experimental mass transfer coefficients with those predicted by the models formulated by Angelo et al and Rose et al. It is found that the data fitted very well when correlated by the model formulated by Angelo et al, therefore it is recommended for mass transfer prediction in agitated columns such as sieve trays.

%85

List of Contents

Content	Page
Dedication.....	i
Acknowledgement.....	ii
Abstract.....	iii
Arabic Abstract.....	v
List of Contents.....	vi
List of Tables	viii
List of Figures.....	x
Nomenclatures.....	xi
Chapter One.....	
1.1 Introduction.....	1
1.2 Stable Drop size.....	3
1.3 Drop Size Distribution in Agitated Systems.....	3
1.5 General objectives.....	5
1.6 Specific objectives.....	5
Chapter Two.....	6
2.1 Droplet Phenomena	6
2.2 Drop Formation:	6
2.3 Droplet Break-up	9
2.4 Droplet Coalescence.....	10
2.4.1 Coalescence Fundamentals.....	11
2.4.2 Drop-Interface Mechanism	11
2.4.3 Drop-drop coalescence Mechanism	13
2.5 Drop Size Distribution	15
2.6 Mass Transfer Fundamentals	18
2.7 Mass Transfer During Drop Formation	19
2.8 Mass Transfer During Drop Travel through the Continuous Phase	21
2.9 Mass Transfer in the Dispersed Phase	22
2.9.1 Stagnant Droplets ...	23
2.9.2 Circulating Droplets:.....	23
2.9.3 Oscillating Droplets:.....	25
2.10 Mass Transfer in the Continuous Phase	27
2.10.1 Mass transfer From and to Stagnant Droplets	28
2.10.2 Mass transfer From and to Circulating Droplets	28
2.10.3 Mass transfer From and to Oscillating Droplets	31
2.11 Mass Transfer During Coalescence	31
2.12 Overall Mass Transfer Coefficients	33
2.13 Application of Single Drop Mass Transfer Models to Agitated Extraction Columns	33

2.14 Mass Transfer and Interfacial Instability	34
2.15 Effect of Surface Active Agent	36
2.16.1 Mass Transfer Models	37
2.16.2 Stage Model.....	39
2.17. behaviour of drops in oil-water Emulsion	41
2.17.1 Analysis of drop	42
2.17.2 Drop size measurement	42
2.18 Equipment Classification.....	42
2.19 Selection of Equipment.....	43
2.20.1 Phase Equilibrium.....	48
2.20.2 Tie-line Correlations.....	49
2.20.3 Othmer and Tobias' Correlation.....	50
2.20.4 Hand's Correlation.....	50
2.20.5 Ishida's correlation.....	51
Chapter Three.....	
3.1 Selection of Liquid-Liquid Chemical Systems.....	52
3.2 Sampling Procedures	52
3.3 Description of Equipment	53
3.3.1 Determination of flooding points:.....	54
3.4 Experimentation	56
3.5 Determination of Equilibrium	56
3.6 Calculation Method	56
3.6.1 Experimental mass transfer coefficient	57
3.6.2 Theoretical mass Transfer Coefficient	59
Chapter Four.....	
4.1 Result	62
4.2 Discussions	88
4.2.1 Column Hydrodynamics	89
4.2.2 Analysis of Results:	90
4.2.3 Experimental mass transfer coefficient	91
4.2.4 Theoretical mass transfer coefficient	91
Chapter Five.....	100
CONCLUSION AND RECOMMENDATIONS	94
5.2 Recommendations.....	95
References.....	96
Appendixes.....	100

List of Tables

Tables	Page
Table (2.1) Factors Affecting Coalescence Time	12
Table (2.2) Comparison between Normal and Log-Normal Distribution Dispersion.....	17
Table (2.3) : Correlation for Mass Transfer During Drop Formation	20
Table (2.4) Correlation for Continuous Phase Mass Transfer Coefficient	30
Table (2.5) 5 Continuous Differential Contactors	45
Table (2.6) Advantages and Disadvantages of Various Contractors	47
Table (4.1).Determination of flooding points at different speeds.	62
Table (4.2) Drop Sizes, number of drops and cumulative volume at 200 rpm. Without mass transfer.....	64
Table (4.3)Determination of Sauter mean diameter (d_{32}),Agitator Speed 200 rpm. Without mass transfer.....	65
Table (4.4) Drop Sizes, number of drops and cumulative volume at 300 rpm. Without mass transfer.....	66
Table (4.5)Determination of Sauter mean diameter (d_{32}),Agitator Speed 300 rpm. Without mass transfer.....	67
Table (4.6) Drop Sizes, number of drops and cumulative volume at 500 rpm. Without mass transfer.....	68
Table (4.7)Determination of Sauter mean diameter (d_{32}),Agitator Speed 500 rpm. Without mass transfer.....	69
Table (4.8) Drop Sizes, number of drops and cumulative volume at 600 rpm. Without mass transfer.....	70
Table (4.9)Determination of Sauter mean diameter (d_{32}),Agitator Speed 600 rpm. Without mass transfer.....	71
Table (4.10) Drop Sizes, number of drops and cumulative volume at 200 rpm. With mass transfer.	72
Table (4.11)Determination of Sauter mean diameter (d_{32}),Agitator Speed 200 rpm. With mass transfer.	73
Table (4.12) Drop Sizes, number of drops and cumulative volume at 300 rpm. With mass transfer.	74
Table (4.13)Determination of Sauter mean diameter (d_{32}),Agitator 300 Speed rpm. With mass transfer	75
Table (4.14) Drop Sizes, number of drops and cumulative volume at 500 rpm. With mass transfer.	76

Table (4.15) Determination of Sauter mean diameter (d_{32}), Agitator Speed 500 rpm. With mass transfer.	77
Table (4.16) Drop Sizes, number of drops and cumulative volume at 600 rpm. With mass transfer.	78
Table (4.17) Determination of Sauter mean diameter (d_{32}), Agitator Speed 600 rpm. With mass transfer.	79
Table (4.18) Mass Transfer Results.	80
Table (4.19) Result of Calculation of V_0 and d_s and d_0	81
Table (4.20) Circulating drop mass transfer coefficient.	82
Table (4.21) Comparison between mass transfer coefficient With calculated for different models.	83
Table (4.22) Comparison between mass transfer coefficient with different operating conditions.	84
Table (4.23) Experimental and theoretical overall mass transfer coefficients.	85
Table (4.24) Comparison between experimental and theoretical mass Transfer coefficients ratio.	86
Table (4.25) Comparison between experimental and theoretical mass Transfer coefficients as percentage.	87

List of Figures

Figures	Page
Fig. (2.1): The relation between drop volume and time of formation	8
Fig. (2.2): : Piston flow model.....	38
Fig.(2.3)): Stage flow model.....	40
Fig. (3.1) Photo pilot plant sieve tray column.....	55
Fig. (3.2) Continuous and Dispersed Phase.....	58
Fig. (4.1) Determinations of flooding points at different speeds of agitation	63

Nomenclatures

The symbols have the following meaning unless otherwise stated in the text:

A	Total interfacial area, cm^2
A	Surface area of an oscillating drop. cm^2
a	Interfacial area per unit column volume cm^2/cm^3
a	Horizontal radius of spheroid
a	Distribution parameter (Skewness parameter)
a_d	Surface area of drop
ΔC	Concentration driving force, gm/cm^3
ΔC_m	Actual mean concentration driving force, g/cm^3
C	Solute concentration, gm/cm^3
C^*	Equilibrium solute concentration, g/cm^3
d	Diameter of drop, cm.
d_o	Mean drop size, cm.
d_{32}	Sauter mean drop diameter, cm.
E	Axial mixing coefficient, cm^2/s
e	Eddy diffusivity, cm^2/s .
F	Constant, Harkins and Brown correlation factor.
g, g_c	Acceleration due to gravity, cm/s^2
H.T.U.	Height of transfer unit, cm.
K	Overall mass transfer coefficient, cm/s .
K_{cal}	Overall theoretical mass transfer coefficient, cm/s .
K_{df}	Mass transfer coefficient during drop formation, cm/s .
K_{exp}	Overall experimental mass transfer coefficient, cm/s .
$K_{o,c}$	Overall mass transfer coefficient of circulating drop, cm/s .

$K_{o.o}$	Overall mass transfer coefficient of oscillating drop, cm/s.
K_a	Overall volumetric mass transfer coefficient, l/s.
K_1, K_2, K_3, K_4	Constants
K_C	Continuous phase mass transfer coefficient, cm/s.
$K_{c.c}$	Continuous mass transfer coefficient of circulating drop, cm/s.
$K_{c.o}$	Continuous phase mass transfer coefficient of oscillating drop, cm/s.
K_d	Dispersed phase mass transfer coefficient, cm/sec.
$K_{d.o}$	Dispersed phased mass transfer coefficient of circulating drop, cm/s.
$K_{d.o}$	Dispersed phase mass transfer coefficient of oscillating drop, cm/s.
K_{HB}	Mass transfer coefficient calculated by means of Handlos and Baron, cm/s.
L	Characteristic dimension of turbulence, cm.
m	Equilibrium distribution coefficient.
N	Rate of mass transfer, gm/s.
$N.T.U.$	Number of transfer unit.
Q	Volumetric flow rate, cm ³ /s.
Q_d	Volumetric flow rate of dispersed phase through nozzle
R_r	Phase flow ratio at inversion.
t	Time, s.
t_f	Time of drop formation, s.
V_o	Vertical relative velocity of drops, cm/s.
V_o	Characteristic velocity of turbulence pulsation
W	Function of oscillating drop characteristics
X	Solute concentration in the raffinate phase, g/100 g.
Y, y	Solute concentration in the extract phase, g/100 g.
Δy_m	Actual mean concentration driving force, g/100 g.

dimensionless groups

F_r	Froude number $\frac{V_c^2}{g_c D_c}$
F_r	Modified Froude number $\frac{V_d^2}{g_c D_c X^2}$
$(Pe)_c$	Peclet number $\frac{V_c H}{E_c}$ for continuous phase.
$(Pe)_d$	Peclet number $\frac{V_d H}{E_d}$ for dispersed phase.
Re	Droplet Reynolds number $\frac{dV_o \rho}{\mu}$
Sc	Schmidt number $\frac{N^2 D_r^3 \rho_c}{\sigma}$
$Sh.$	Sherwood number $\frac{dV_o^2 \rho_c}{\sigma}$
We	Weber number $\frac{P}{\sigma / d}$

Greek letters

α	Back flow coefficient.
α	Constant
γ	Surface tension, dyne/cm.
ε	Amplitude of oscillation.
ε_o	Function of amplitude of oscillation defined
μ	Viscosity, g/cm.s
ν	Kinematics viscosity, cm ² /s.
ν	Cumulative volume of drops, cm ³
ρ	Density, g/ cm ³

$\Delta\rho$	Density difference, g/ cm ³
σ	Interfacial tension, dyne/cm.
τ	Dimensionless time.
φ	Coalescence frequency
ω	Frequency of oscillation, 1/s.
π	Constant = 3.1416.

CHAPTER ONE

INTRODUCTION

1.1 General

The main polluting materials from petroleum processing are hydrocarbons, which due to their properties affect the environment. The removal of oil from water oil/ emulsion must include both oil recovery and treatment of liquid wastes to ensure clean environment. The pollution sources related to petroleum industry are mainly at the production fields, during transportation and during refining. During off shore production the formation water pumped with the oil contains a considerable amount of oil when settled and separated. Oils spliges from sea accidents during transportation, tankers cleaning waters and during refining from desolaters, condensers and cracking units all contribute considerably to pollution.

Mechanical processes which do not use any reagent, such as demulsifiers, coagulants or flocculants are applied to collect the hydrocarbons. Oil separation by settling is based on the existence of an upward velocity of the ascending oil droplets through the water due to specific gravity of oil being lower than that of water. This velocity is governed by Stokes's law which correlates the diameter of the droplet, the densities and viscosity of the liquid at the prevailing temperature. Oil collectors are used to collect oil already gathered on the surface of water, they are either statically or dynamically operated. However, all these methods of separation and oil collection are designed to collect oil slicks at the surface of the water and they cannot, whatsoever, perform a deep oil removal in the water. Hence, a method that can recover or extract the oil at all vicinities in oil/water waste needs to be developed.

Usually primary treatment processes are used to screen out most solids, to reduce the size of the solids and to separate floating oils. The secondary treatment follows the primary treatment to remove organic

matter through biochemical oxidation, Hanson (1975) A particular biological process selection depends on the quantity of waste water, biodegradability of waste, and land area. Activated sludge reactors, and tricking fitters are commonly used.

A tertiary treatment is proposed in this study to recover the oil after the primary and secondary processes. The proposed process depends on the ability of a highly selective solvent to extract the hydrocarbon oil from oil/water emulsion. This process is capable to allow both the solvent and emulsion to get into intimate contact and as the hydrocarbon is completely miscible with the solvent, it will be separated and recovered.

The crude oil in oil fields when pumped out from a well contains a lot of water, and therefore it is introduced into settling tanks to separate the oil from water by gravity settlement. Nevertheless, the water separated still contains an appreciable amount of oil and needs to be treated to separate this oil. The process of separation of the oil in this waste water is difficult due to its smaller quantity. If such waste of oil/water is drained in open areas, it will affect the environment and the ecology of all premisses where it may be disposed thereto. So the aim of this study is to develop an efficient method of separation of waste oil/water dispersion.

It is known that crude oil is completely immiscible with water and therefore it can not be considered as a solute as the case in solvent extraction unless it is emulsified. It may be separated through a highly selective solvent which must also be completely immiscible with water. The small amount of oil and big quantity of water must first be dispersed into small droplets counter-currently with the solvent. These droplets when get into contact with the solvent, they will coalesce, mix with the solvent and thus separated and transferred with the solvent up through the column.

The process of dispersion of oil in water is governed by the speed of agitation, the higher the speed the smaller the drop size and the better is the dispersion. Thus when two immiscible liquids are agitated, a dispersion is formed in which continuous break-up and coalescence of droplets occur until a dynamic equilibrium is established between the break-up and coalescence process. But, when a high selective solvent is present, the droplets that have been coalesced would mix with that solvent and thereby separated.

For this reason a solvent of high selectivity towards the crude oil such as n-hexane is selected and used. The separation depends upon the type and the extent of agitation and the physical properties of the liquids. If the extent of agitation is sufficient to maintain a uniform level of turbulence throughout the column, the mean drop size and drop size distribution will be the same throughout. The factors that affect the break-up and coalescence of drops will be investigated in this study as well as the column hydrodynamics such as flooding. However, for every physical system and set of conditions, there must be a stable drop size. Drops larger than this size will tend to break-up whereas smaller drops will tend to coalesce.

1.2 Stable Drop Size

In any physical system, the stable drop size depends on the extent of the turbulence. Thus, when a drop existing in a field of homogenous isotropic turbulence, the forces acting on the drop will be the dynamic forces due to the turbulence eddies attempting to break-up the drop and these will be opposed by the surface forces attempting to resist break-up, and when the two forces are equal the drop will be stable.

1.3 Drop Size Distribution in Agitated Systems

In most situations involving the agitation of immiscible liquids the dispersed phase hold-up is such that the mean drop size and drop size distribution is affected by droplet coalescence. A high turbulence increases the frequency with which drops collide, thereby increasing the probability of coalescence. The inter-droplet coalescence is of fundamental importance, not only in relation to drop size in agitated columns, but also believed that repeated break-up and coalescence enhance extraction

The oil in waste oil/water may be found at the surface in very small quantity, some of it may be in between the molecules of water, therefore it is very important to be emulsified. The emulsification makes the oil partially soluble in water and makes it well distributed and easily extracted. A dispersant is a detergent which is oil soluble surface active material, capable of maintaining the oil in stable emulsion and partially soluble in water, Hanson(1975)

The process entails the dispersion of the oil as droplets into a continuous phase followed by the oil transfer from the droplets to the solvent phase when the drops coalesce and mixed with it. Liquid-liquid extraction is selected because it is impractical to make the separation through distillation for such a very diluted oil/water emulsion. Following extraction it is necessary to recover the oil and the solvent and this process

may entail fractional distillation. Any extraction process may involve the following:

- a) The solvent and the solute in the mixture must be brought into intimate contact.
- b) The two phases must be separated.
- c) Recovery of the solute and solvent.

A wide variety of equipments can be used for such separation in either a continuous manner using packed, RDC, spray Scheibel columns, or in stage-wise manner such as sieve tray or mixer – settler.

A wide distribution of droplet size exists in separation contactors, dependent upon the degree of turbulence which leads to break-up and re-coalescence effects. The mass transfer rate from and to the drops is different and depends on the type of a drop and whether it is stagnant, circulating or oscillating. Recently agitated columns involving pulsing or agitation have much been applied. These type of equipments offer the advantage of flexibility, high efficiency and reasonable volumetric capacity AL-Saadi (1979)

1.4 Statement of the problem

The Sudan is now an oil producing country. The production of both crude oil and refined products produce a lot of liquid wastes such liquid wastes are contaminated with oil and need to be purified. The method of purification in application are not efficient and this is why the treated water is not recycled , instead, it is left to be evaporated in pools causing a serious environment problem.

The aim of this study is to purify the treated water in order to remove every traces of oil by solvent extraction. A sieve tray agitated column and n-hexane solvent are suggested for the extraction process.

1.5 General objectives

1. Treatment of liquid petroleum for reused and recycling .
2. Selection of a suitable solvent for extraction of oil droplets.
3. Study of columns performance with regard to column hydrodynamics.

1.6 Specific objectives

1. To study the column hydrodynamics and its effectiveness on separation of oil droplets.
2. To investigate and compare the mass transfer coefficients against those calculated by various models.

CHAPTER TWO

LITERATURE REVIEW

2.1 Droplet Phenomena

The phenomena of ‘coalescence-redispersion’ is highly pronounced in the agitated columns. It significantly controls the hydrodynamics and mass transfer characteristics of the column. Thus a fundamental understanding of drop interaction. i.e., drop break-up and coalescence phenomena is important in the context of the present work.

In a continuous counter-current extractor the dispersed phase may be introduced into the continuous phase via a distributor in an attempt to obtain a uniform initial drop size distribution. However, despite careful design of the distributor, with equi-sized sharp-edged perforations, a wide range of drop sizes are observed in all agitated counter-current contractors. This drop size distribution in the agitated column results from the coalescence-redispersion mechanism arising from the application of the external energy.

In studies with a variety of organic liquid dispersed in water in a pilot scale agitated columns it was found that, in the absence of mass transfer, inter drop coalescence was negligible until flow rates approach the flooding. Hence in the absence of any special interfacial effects associated with mass transfer the column appears to function as a discrete drop contacting device. However, both the break-up and formation mechanisms, and interdroplet phenomena merit consideration since they are fundamental to the understanding of how columns operation.

2.2 Drop Formation:

The rate of mass transfer in any liquid-liquid system is affected by the rate of the formation of the droplets, their rate of passage through the continuous phase and finally their rate of coalescence. The regime of drop

formation in the agitated columns is independent on agitator speed and hold-up, but only on the linear velocity of the dispersed phase through the distributor.

The volume V_f of drop released from a nozzle may be presented as a function of the time of formation t_f , in the form shown in figure 2.6 (Heertjes 1971). In region (I) the drop volume, V_{\min} , is independent of the time of formation, and can be estimated with fair accuracy by a method by Harkins and Brown (1991). Region (II) has been the subject of extensive studies and many correlations have been proposed, e.g., those of Treybal and Howrth (1950) and Null and Johnson (1958). However, both correlations have been found to be unsatisfactory over a wide range of liquids properties and nozzle geometries Meister (1966). Probably the most satisfactory correlation for predicting drop size is that proposed by Scheels and Meister, (1966). This has the form:

$$V_f = F \left[\left(\frac{\pi \sigma D_N}{\Delta \rho g} \right) + \left(\frac{20 \mu c Q D_N}{d_f^2 \Delta \rho g} \right) - \left(\frac{4 \rho_D Q U_N}{3 g \Delta \rho} \right) + 4.5 \left[\frac{Q^2 D_N^2 \rho d \sigma}{(g \Delta \rho)^2} \right]^{\frac{1}{3}} \right] \quad (2.1)$$

where F is the Harkins-Brown (1991) correction factor, which can be estimated from a plot of F VS. Little work has been published regarding region (III) in which jetting from the nozzle, becomes apparent in region (IV) jetting is fully developed and drop formation takes place at the end of a Rayleigh jet(1971).

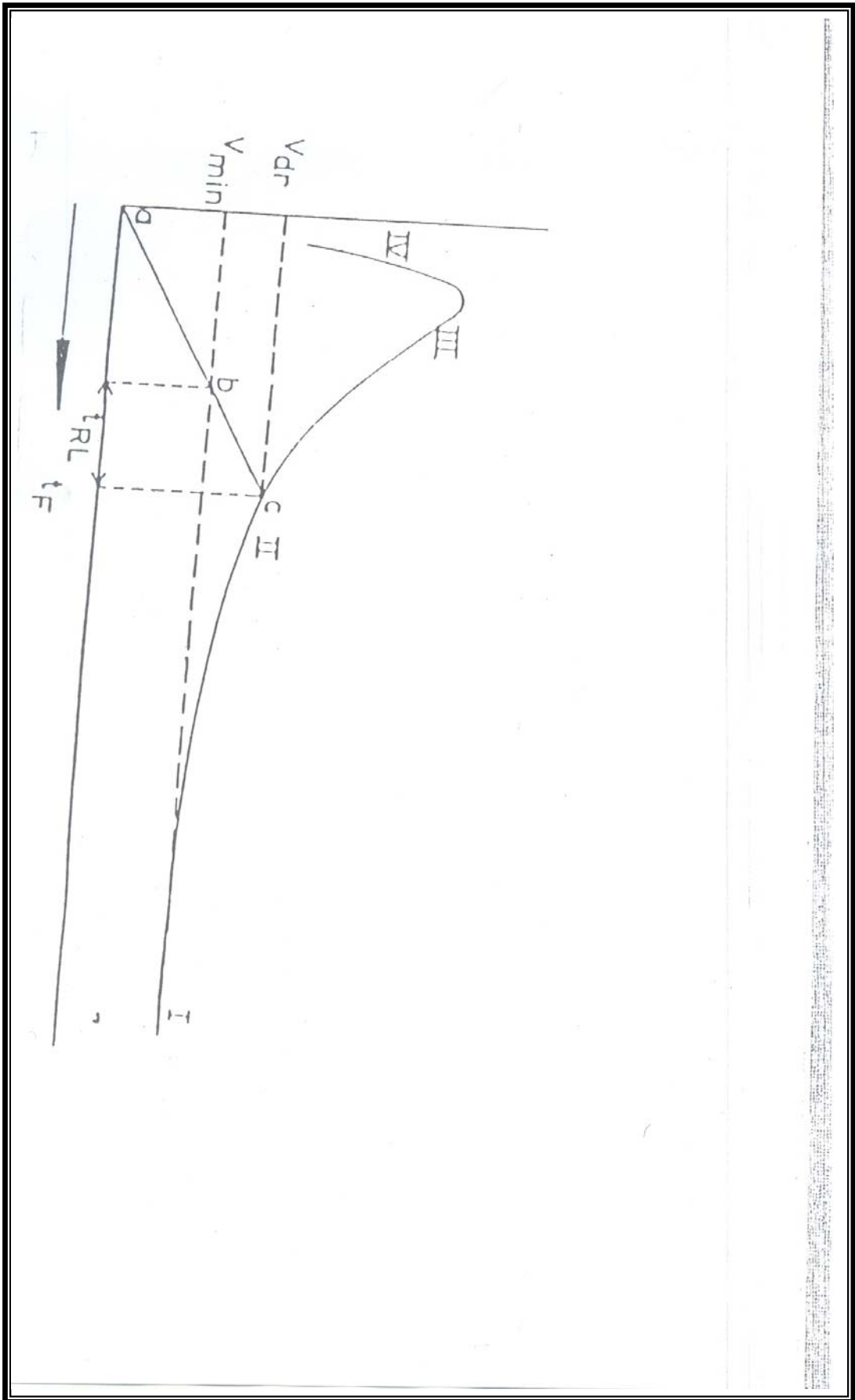


Fig (2.1):The relation between drop volume and time of formation

2.3 Droplet Break-up

In turbulent systems deformation of drops is caused by various interacting forces e.g. energy transmitted by the impeller or impact against the container walls and internals, or impact between drops.

In an agitated liquid-liquid system, droplets break-up occurs when:

- (a) the magnitude of the dynamic pressure acting upon a drop, surpasses the magnitude of the cohesive surface forces, and
- (b) the droplet stays in the high shear zone for sufficient period of time.

Kolmogoroff (1941) first studied turbulent flow in a stirred tank and developed a theory of local isotropy. This postulated that in turbulent flow instabilities in the main flow amplifies existing disturbances and produces primary eddies which have a wavelength, or scale, similar to that of the main flow. The large primary eddies are also unstable and disintegrate into smaller and smaller eddies until all their energy is dissipated by viscous flow, Hinze (1955) considered the fundamentals of the break-up process and characterized them by two dimensionless groups.

$$(1) \text{ Weber number } N_{we} = \frac{P}{\sigma/d} \quad (2.2)$$

$$(2) \text{ Viscosity group } N_{vi} = \frac{\mu d / d}{(pd\sigma/d)^{1/2}} \quad (2.3)$$

Deformation increases with increasing N_{ew} until, at a critical N_{ew} , break-up to result from viscous stresses the drop must be small compared to the region of viscous flow Minz(1955). Break-up due to dynamic pressure fluctuation have been considered by Hinze(1959). In this regime, changes in velocity over a distance equal to the drop diameter cause a dynamic pressure to develop; this pressure determines the magnitude of the largest drop pressure, Hinze (1955) extended Kolmogoroff's (1941) energy distribution to predict the size of the maximum stable drop in a turbulent field as

$$d_{\max} = C \left(\frac{g_c \rho}{\rho_c} \right)^{\frac{3}{5}}, \quad \bar{c}^{-2/5} \quad (2.4)$$

where C is a constant. The value of C was calculated as 0.725 based on an analysis of the rotating cylinder data of Clay (1940). Strand et al (1962) suggested that the coefficient C can be adjusted to match specific conditions accompanying mass transfer and the tendency of drops to coalesce and break-up.

2.4 Droplet Coalescence

Coalescence phenomena is important to the hydrodynamics of any extraction column, since interdrop coalescence in the agitated zone is one factor determining the equilibrium drop size generated in the column and coalescence is required at the interface near the dispersed phase outlet to achieve phase separation. Within the agitated zone the drop size is determined by a balance between break-up and coalescence. This size determines the interfacial area and drop rise velocity. The height of the dispersed phase separation zone depends on the case with which phase coalescence occurs at the interface. This is also a function of the drop size generated.

The coalescence rate depends on the system properties, drop size and coalescence mechanism. There are three separate mechanisms of coalescence in any column.

- (i) Drop interface coalescence
- (ii) Drop-drop coalescence.
- (iii) Drop-solid surface coalescence.

Mechanism (I) always occurs in the setting section where phase separation takes place. Mechanism (ii) usually occurs in the mixing section, as well as in the settling section when a layer of uncoalesced drops accumulates. Mechanism (iii) is a special case of drop coalescence on the

column internals and/or the column wall, if it is wettable by the dispersed phase.

2.4.1 Coalescence Fundamentals

In general, coalescence is a simple fusion of two or more macroscopic quantities of the same substance. Coalescence took place because the free energy associated with the large interfacial area between the phases can be decreased by aggregation or coalescence of the dispersed phase droplets. From energy balance considerations coalescence of a liquid dispersion would be expected until ultimately two layers are formed. Coalescence generally occurs in three steps.

- (i) Flocculation of drops.
- (ii) Collision and drainage of the continuous phase film until it reaches a critical thickness.
- (iii) Rupture of the film.

The coalescence time depends on the drainage and rupture of the continuous phase film, factors affecting these steps control the coalescence process. These factors have been well documented by Lawson(1967), some of these factors are summarised in table 2.1.

2.4.2 Drop-Interface Mechanism

Coalescence of single drops at a plane interface consists of five distinct steps: Lawson et al(1967)

1. Approach of the drop to the interface and the subsequent deformation of the drop and interface profiles;
2. The damping of oscillations caused by the impact of the drop at the interface;
3. Formation and drainage of a continuous phase film between the drop and its bulk interface;
4. Bupture of the film; and

5. Drop contents desposition into the interface

Table 2.1 Factors Affecting Coalescence Time

Variable (increasing)	Effect on coalescence time	Explanation in terms of effect on continuous film drainage rate
1. Drop size	Increase	More of the continous phase film
2. Distance of fall	Increase	Drop ‘bounces’ and film is replaced
3. Interfacial tension	Decrease	More rigid drop, less continuous phase in films
4. Phase	Increase	More drop deformation, more continuous phase in film
5. Phase viscosity ratio	Decrease	Either less continuous phase in film or higher drainage rate
6. Temperature	Decrease	Increase phase viscosity ratio
7. Temperature gradients	Decrease	Film distorts
8. Curvature of interface towards drop:		
a) concave	Increase	More continuous phase in film
b) convex	Decrease	Less continuous phase in film
9. Presence of a third component		
a) surfactants	Increase	Forms ‘skin’ around drop, film drainage inhibited
b) mass transfer into drop	Increase	Sets-up interfacial tension gradients which oppose film flow
c) mass transfer out of drop	Decrease	Sets-up interfacial tension gradients which assist flow of film

The sum of steps 1 and 2 is referred to as the pre-drainage time. This is generally of the order of 0.1 seconds and step 5 as post-drainage step which takes about 0.05 seconds. Thus coalescence time may be considered as the sum of the times taken by steps 3 and 4 and can be of order of several seconds.

A distribution in the coalescence time for identical drop sizes has been reported in many investigations Gillespie et al (1956). This distribution has been found to be approximately Gaussian.

Although a number of correlations for coalescence time have been proposed by various workers in terms of the ratio of number of drops not coalescing in time t to the total number of drops examined, controversy has arisen over their validity and reproducibility Jeffreys(1971). This is probably because studies have been carried out under varying conditions Cockbain et al(1953). Presence of electrolytes or surfactants is expected to affect the interfacial tension which in turn may reduce or increase the film drainage process.

2.4.3 Drop-drop coalescence Mechanism

Inter droplet coalescence occurs frequently in mixing section of the agitated contactors like the plate column and Oldshue Rushton column though the effect is more pronounced in the latter.

The analysis of drop-drop coalescence which represents a more dynamic situation in agitated systems is rather difficult on two counts. Firstly, it is difficult to reproduce a controlled collision between two drops which have not been restrained in some way. Secondly there is an inherent randomness in the manner in which the drops rebound or coalesce. Thus drop-drop coalescence studies necessitate consideration of both collision theory and the coalescence process. It follows that the prediction of

coalescence frequency requires a knowledge of both collision frequency and coalescence probability.

From the above consideration and using a purely theoretical approach, Howarth(1966) developed an equation to relate the frequency of coalescence with dispersed phase hold-up in a homogeneous isotropic turbulent flow.

$$\phi = \left[\frac{24XS\bar{V}^2}{d^3} \right] \exp \left[-\frac{3V^{*2}}{4V^2} \right] \quad (2.5)$$

where ϕ is coalescence frequency, V^2 is the mean square Lagrangian turbulent velocity fluctuation, V^* is the critical approach velocity. Although this equation showed good agreement with Madden and Damerell's (1962) observation for water drops dispersed in toluene in an agitated tank, doubt has been expressed as to the applicability of Howarth's model to real situations due to the restrictive assumptions made in the derivation.

In a later study, Misck (1964) characterised the dispersion by hydraulic mean drop diameter and assumed that these drops exactly followed the tubulent fluctuations in the continuous phase. Every collision of droplets was assumed to result in coalescence. Since drop-drop coalescence can take place, either in the ublk of liquid or at the wall of the column, Misek (1964) proposed a different correlation for each case. For coalescence in the bulk of the fluid.

$$\begin{aligned} \ln \frac{d}{d_0} &= K_1 (n_0 d^3) \mathcal{V}_0^{0.5} \left(\frac{D_c \mathcal{V}}{\mu} \right)^{0.5} = K_2 X \left(\frac{\sigma}{d_0 \rho} \right)^{0.5} \left(\frac{D_c \rho}{\mu} \right)^{0.5} \\ &= Z_1 X \end{aligned} \quad (2.6)$$

and for coalescence at the column wall.

$$\ln \frac{d}{d_0} = K_3 (n_0 d^3) \mathcal{V}_0 \left(\frac{D_c \rho}{\mu} \right) = K_4 X \left(\frac{\sigma}{d_0 \rho} \right)^{0.5} \left(\frac{D_c \rho}{\mu} \right) = Z_2 X \quad (2.7)$$

The values of Z_1 and Z_2 were determined indirectly based on phase flow-rate measurements using Miskel's equation. Only a fair agreement was obtained with the above equations when they tested experimentally for a number of binary systems in various agitated columns like the R. D. C., Oldshue-Rushton column and Scheibel column. A value of 1.59×10^{-2} for the constant K_2 in Equation 2.6 was claimed to be independent of the type of mixer. However, it is doubtful whether coalescence characteristics in columns as different in Operation as the R.D.C. and Oldshue-Rushton can properly be represented by a single operation Mumford(1970). Furthermore, the equations make no allowance or the known variation in the case of coalescence with drop size.

Drop coalescence with solid surfaces is strictly a case of “wetting properties”.

2.5 Drop Size Distribution

In all practical liquid-liquid contacting devices, the dispersed phase exists predominantly as discrete drops. In order to analyse extraction data the assumption commonly made is that these drops are spherical and of uniform size. This permits the use of a discrete drop size in the mass transfer calculations. Olney(1964) and Stainthorp et al (1964) reported that such assumption may lead to serious errors due to the fact that there is a distribution of mean drop size along the column length. If there is a large range of drop sizes in a column the drop size distribution $f(d)$ must be included in the analysis.

In most agitated contractors drop size distribution is a result of the competing effects, viz., the generation of new drops by break-up due to shear or local turbulence in the bulk flow, and of droplet coalescence due to the interaction effects madden et al (1962). This size distribution is bounded by an upper limit or maximum stable drop size Hinze (1955) which in the absence of coalescence will be determined by the size of the

nozzles, and a lower limit or minimum size, dependent upon the prevailing break-up processes. This minimum size, may be dictated by the size that is just entrained by the continuous phase Olney (1964).

There is a considerable disagreement over the shape of the drop size distribution curve in an agitated system some investigations report a normal distribution Bouyatiotis et al (1967), while others found the distribution to be log-normal. This is of practical significance in the analysis of the performance of an extraction column. Thus for a fixed volumetric throughput, a comparison of the two types of dispersion is given in Table 2.2 shows that a normal distribution, where the mode is equal to the mean, results in more drops being nearer to the mean size would be preferable to a log-normal distribution for predicting the characteristics of an extraction column. However, Chartes and Korchinsky(1975) confirmed Olney's (1964) conclusion that the drop size distribution in a plate column obeys the upper limit distribution proposed by Mugele and Evans (1951)

$$\frac{dv}{dr} = \frac{\varepsilon}{\sqrt{\pi}} \exp(-\delta^2 r^2) \quad (2.8)$$

where $r = \ln\left(\frac{a'd}{d_m - d}\right)$ (2.9)

The upper limit distribution is modified log-normal distribution which may be compared with the standard form of the log-normal distribution

$$\frac{dv}{dr} = \frac{\varepsilon}{\sqrt{r}} \exp(-\delta^2 r^2) \quad (2.10)$$

where $r = \ln \frac{d}{d_{vg}}$ (2.11)

where d_{vg} is the geometric mean drop diameter.

Table 2.2 Comparison between Normal and Log-Normal Distribution Dispersion

Property of Dispersions	Normal Distribution	Log-normal distribution
Proportion of smaller droplets	Lower	Higher
Mean mass transfer coefficient	Higher because more drops are circulating	Lower-more stagnant drops
Interfacial area	Lower	Higher
Tendency to flood column	Higher	Lower
	Lower	Higher

Chartres and Korchinsky(1975) have shown that Olney’s (1964) data are accurately represented by the upper limit distribution rather than the log-normal distribution. In addition Korchinsky and Azimzadeh-Khateylo (1976) found that the upper limit distribution accurately represented the drop size data in an Oldshue-Rushton column. They emphasised the importance of applying drop size distribution in the mass transfer calculation instead of using the Sauter mean diameter (d_{32}). Olney (1964) has also shown that d_{32} may not be the proper mean drop size to represent the transfer rate for the total drop population and concluded that the upper limit distribution will represent the drop size distribution in a plate column. In another study Chartres and Korchinsky(1978) stated that the size of sample drops used to represent a dispersion is also extremely important. They also point out the marked effect of inlet drop size on column drop size and measured extraction efficiency. Finally study, Jeffreys, and Mumford also confirmed the accurate representation of the upper limit density distributions of Mugele and Evans (1951) for the drop samples in large plate column. They compared the Sauter mean diameter d_{32} calculated by the volume-surface diameter equation.

$$d_{32} = \frac{\sum nidi^3}{\sum nidi^2} \quad (2.12)$$

and d_{32} calculated by the following equation

$$d'_{32} = -\frac{d_m}{1 + a'e^{0.25}\sigma^2} \quad (2.13)$$

Both d_{32} and d'_{32} were in a very good agreement.

2.6 Mass Transfer Fundamentals

The rate of mass transfer in all extraction equipment depends on the overall mass transfer coefficient, the interfacial area, and the driving force. The overall mass transfer coefficient depends on the rate of diffusion inside, across the interface and outside the droplet. Therefore the mechanism of solute transfer from or to a single drop is fundamental to the overall transfer process in practical equipment.

In considering mass transfer, the life span of a droplet inside a contractor may be divided into three stages

- (i) formation time at the distributor,
- (ii) travel time through the continuous phase,
- (iii) coalescence time at the bulk interface in the separation zone,

mass transfer occurring, to some degree, at each stage, in agitated columns the magnitude of contributions from (i), (ii) and (iii) will be dependent on the rate and frequency of droplet coalescence and re-dispersion.

2.7 Mass Transfer During Drop Formation

Various workers have measured the extent of mass transfer during drop formation, Sherwood (1939) observed that 40% of the overall transfer occurred during the formation period, but investigations by Jeffry's et al, (1962) has shown that the amount is to be around 10%. However, Sawistowski, (1963) has shown that the prediction of precise extraction rates during drop formation is difficult because of the rapid changes in interfacial tension, and the interfacial area of the droplet, which occur during this period. Nevertheless, many mathematical expressions have been proposed to predict dispersed phase mass transfer coefficient during drop formation. These are summarized in Table (2.3) . Gurashi (1985).

Skelland and Minhas, (1971) concluded that the these models are unrealistic because they fail to allow for the effects of internal circulation, interfacial turbulence and disturbances caused by detachment. A modified expression was proposed for the mass transfer coefficient, which is:

$$K_{df} = 0.0432 \left(\frac{d}{t_f} \right) \left(\frac{V_n^2}{dg} \right)^{0.089} \left(\frac{d^2}{t_f D_N} \right)^{-0.334} \left(\frac{L_d}{\sqrt{D_d d \sigma}} \right)^{-0.601} \quad (2.14)$$

Where:

K_{df} : mass transfer coefficient during drop formation.

d : diameter of drop.

t_f : time of drop formation.

V_n : characteristic drop of velocity.

L_d : characteristic dimension of turbulence.

D_N : nozzle inside diameter.

Table 2.3: Correlation for Mass Transfer During Drop Formation

Authors and References	Correlation
------------------------	-------------

Licht and Penshing (1953)	$K_{df} = \frac{6}{7} \left(\frac{D_N}{\pi \tau_f} \right)^{0.5}$
Heertjes et al (1954)	$K_{df} = \frac{24}{7} \left(\frac{D_N}{\pi \tau_f} \right)^{0.5}$
Groothuis et al (1955)	$K_{df} = \frac{4}{3} \left(\frac{D_N}{\pi \tau_f} \right)^{0.5}$
Coulson and Skinner (1951)	$K_{df} = 2 \sqrt{\frac{3}{5}} \left(\frac{D_N}{\pi \tau_f} \right)^{0.5}$
Heertjes and de Nie (1966)	$K_{df} = 2 \left[\frac{r_0}{a_d} + \frac{1}{3} \right] \left(\frac{D_N}{\pi \tau_f} \right)^{0.5}$
Heertjes and de Nie (1991)	$K_{df} = \frac{14}{3} \left[\frac{\bar{r}_0}{a_d} + \frac{1}{3} \right] \left(\frac{D_N}{\pi \tau_f} \right)^{0.5}$
I Ikovic (1939)	$K_{df} = 1.31 \left(\frac{D_N}{\pi \tau_f} \right)^{0.5}$
Angelo et all (1971)	$K_{df} = \frac{2}{\tau} \left(\frac{D_N}{\pi \tau_f} \right)^{0.5}$

These correlations represent the overall mass transfer occurring during formation, which includes mass transfer during drop growth, during the detachment of the drop and the influence of the rest drop. Around 25% Rod (1971) deviation was observed from the experimental values. This model did not however consider the rate of formation as one of the variables affecting mass transfer, whereas Heertjes et al (1966) and Coulson and Skinner, (1951) observed higher frequencies of drop formation.

The following expression for mass transfer prediction .

$$E_F V_d = \frac{4n}{2n+1} \int_0^1 (1-y^2) dy \cdot (C^* - C_0) \left(\frac{D_n}{n} \right)^{0.5} B_p t^{(2n+1)/2} \quad (2.15)$$

where n and B_p are defined by the surface area $A = B_p t^n$ and $y = (1-t/t_1)^2$, t is the time at which a fresh surface element is formed and t_1 that when mass transfer is considered. The above model is applicable to drops with a moderate rate of formation given by.

$$1.28 \times 10^4, \left(\frac{d^2}{t_f D_N} \right), 12.31 \times 10^4$$

In case of formation at high speed, i.e., $Re > 40$, large contributions to mass transfer are caused by strong circulation in the drop. For low rates of formation mass transfer in these circumstances is comparable to that with drops formed at moderate speed on which is superimposed the contribution of free convection Heertjes, (1971).

2.8 Mass Transfer During Drop Travel through the Continuous Phase

Mass transfer during drop travel through the continuous phase is significantly influenced by the hydrodynamic state of the drop, i.e. whether it is stagnant, circulating or oscillating. The mechanism of transfer differs in each case. Circulation or oscillation induces intense mixing inside the drop. Conversely, a rigid or stagnant drop, in which internal mixing is completely inhibited, has a lower mass transfer rate. Oscillations commence in regimes of flow for which droplet Reynolds number is > 200 . Below this circulation predominates Rose et al, (1966). Good agreement, however, has often been found between the rates of mass transfer for oscillating drops and those with rapid internal circulation, but in several instances Angelo et al (1966), the rates were considered to be much higher for oscillating drops. Although mass transfer is dependent on the hydrodynamic state of the drops, the presence of a wake behind the moving drop may considerably affect the overall transfer rate Forsyth et al, (1974). Few attempts have been made to quantify this effect which may be pronounced in quiescent flow. Kinard et al, and Garner et al (1960) developed an equation to modify the driving force due to entrainment of a

wake behind the drop. while Forsyth et al (1974) proposed a theoretical analysis of the effect in spray columns. Wake phenomena have little significance in turbulent flow systems, because the continuous phase is continually renewed and the wake is not allowed to develop.

2.9 Mass Transfer in the Dispersed Phase

In agitated columns the proportion of mass transfer which occurs during droplet travel would be expected to be very much greater than during release or detachment from the inlet distributor. The coefficient of mass transfer inside the droplet depends on the degree of internal circulation. Circulation rate is known to increase with the droplet diameter and with the ratio of the viscosity of the continuous phase to that of the dispersed phase. Hadamard(1911) showed that the liquid inside the droplet would circulate at droplet's Reynold number greater than 1.0, and Levich et al (1949) postulated that circulation would occur between Reynolds number of 1.0 and 1500. Garner et al (1955), considered that the surface tension of the dispersed phase would affect the circulation rate. Later Al-Hassan, (1974) showed that Reynolds number alone is insufficient to explain the hydrodynamic state of the drop. And that all properties have to be considered in addition to Reynold number. Droplet Reynold number, however, may be used as a rough guide to determine the hydrodynamic state of the drops as following:

- (i) stagnant droplets or rigid droplets when $Re < 1.0$,
- (ii) circulating droplets when $1.0 \leq Re < 200.0$
- (iii) oscillating droplets when $Re \geq 200$.

Pure liquid systems with different properties produce drops with widely different mass transfer characteristics. The range of behaviour from stagnant drops to oscillating drops are therefore considered in details below.

2.9.1 Stagnant Droplets

These are generally very small droplets, usually less than 1.0 mm in diameter, with no internal circulation and molecular diffusion is considered to be the dominant mechanism. For the case of no resistance to mass transfer in the continuous phase, this situation is adequately represented by the (Newman's 1931) relation:

$$E_m = \frac{C_0 - C_f}{C_0 - C^*} = 1 - \frac{6}{\pi^2} \sum_{n=1}^{\infty} \frac{1}{n^2} \exp\left(\frac{-n^2 \pi^2 D dt}{r^2}\right) \quad (2.15)$$

Vermulen (1953) found that Newman's model could be closely approximated by the empirical expression:

$$E_m = \left[1 - \exp\left(\frac{-\pi^2 D dt}{r^2}\right) \right]^{-0.5} \quad (2.17)$$

which for values of E_m less than 0.5 reduces by a series expansion neglecting higher order terms to :

$$E_m = \pi \left(\frac{D dt}{r^2} \right)^2 \quad (2.18)$$

correlation for the mass transfer coefficient based on a linear concentration-difference driving force is proposed by (Treybal (1963) as:

$$K_d = \frac{4\pi^2 D_d}{3r} \quad (2.19)$$

2.9.2 Circulating Droplets:

The circulating droplets are those in which the fluid inside the drop is in a state of rapid circulation. This circulation is laminar at droplet Reynolds numbers less than 1.0 and turbulent at Reynolds number greater than 1.0. as a result of these phenomena, the fluid inside the drop is completely mixed and this results in a higher mass transfer coefficient.

A theoretical analysis of mass transfer inside a circulating droplet with laminar circulation has been made by Kroning and Brink(1960). They assumed that circulation rate was sufficiently rapid to maintain the

streamlines at constant, but different concentrations. Hence mass transfer occurs by molecular diffusion in a direction perpendicular to the streamlines. The rate of mass transfer inside circulating drops was shown to be far greater than in stagnant drops. They proposed a correlation for a droplet in this situation neglecting the resistance to mass transfer in the continuous phase

$$E_m = 1 - \frac{3}{8} \sum_{n=1}^{\infty} A_n^2 \exp\left\{-\lambda_n \frac{16D_{dt}}{r^2}\right\} \quad (2.20)$$

where A_n and λ_n are eigenvalues Heertjes et al (1954) presented values for A_n and λ_n values of n from one to seven Calderbank et al(1956) proposed an empirical approximate to equation 2.6 as:

$$E_m = 1 - \exp\left(\frac{2.25D_{dt}}{r^2}\right) \quad (2.21)$$

An approximate expression for the mass transfer coefficient was also proposed by Kronig and Brink (1960) for circulating droplets under laminar circulation as:

$$K_d = \frac{17.9D_d}{d} \quad (2.22)$$

Alternatively, Handlos and Baron (1957) considered the case of a fully turbulent drop, with circulation pattern simplified to concentric circles. It was assumed that the liquid between two streamlines became really mixed after one circuit. They proposed a correlation for mass transfer coefficient for droplets under turbulent circulation as:

$$K_d = \frac{0.00375 V_t}{1 + \mu_d / \mu_c} \quad (2.23)$$

Equation 2.23 has been verified experimentally, by Skelland and Wellek (1964) and Johnson and Hamilec (1960) However Olander (1966) observed some deviation when applying the Handlos and Baron model to cases involving short time of contact. This is due to the fact that, in the derivation of equation 2.23, only the first term of the series which appeared

in the mathematical evaluation has been used Olander (1961). This is permissible only when the contact times are large. Thus Olander(1966) proposed a correlation for the actual mass transfer coefficient k as

$$K_d = 0.972k_{HB} + 0.075\frac{d}{t} \quad (2.24)$$

where K_{HB} is the mass transfer coefficient calculated by means of Handlos and Baron's model. Equation 2.24 is applicable for cases where there is no resistance in the continuous phase.

2.9.3 Oscillating Droplets:

When a droplet reaches a certain size it begins to oscillate about an ellipsoidal shape. This usually happens when the drop Reynolds number exceeds 200 in a continuous phase of low viscosity. The cause of the onset of this oscillation is subject to many investigations. However, Gunn (1949) suggested that oscillations would occur when the periodic force produced by the detachment of wake eddies had the right frequency to self excite vibrations. As droplet size increases beyond the point where oscillations begin, the droplet oscillation tends towards a more random fluctuation in shape Rose et al. (1966).

Garner and Tayeban, (1960) found that for a given droplet size oscillation was greater for systems with a low continuous phase viscosity, a low interfacial tension and a low dispersed phase viscosity. Garner and Haycock (1959) found that the period of oscillation was dependent on the physical properties of the liquid-liquid system, particularly the densities. Johnson and Hamielec(1960) reported that once oscillations were set up in drops, the effective diffusivities are as high as 52 times the molecular value. Garner and Skelland (1955) reported that the rate of mass transfer of an oscillating nitrobenzene drop in water was 100% greater than that for an equivalent stagnant drop. Rose and Kinter(1966) proposed a model for

mass transfer from vigorously oscillating, single liquid drops moving in a liquid field based upon the concept of interfacial stretch and internal droplet mixing. Their model takes into account both an amplitude factor and the frequency of drop oscillations. They stated that oscillations break-up internal circulation streamlines and turbulent internal mixing is achieved. The proposed model gives

$$E_m = 1 - \exp \left[\frac{-2\pi D_E}{V} \int_{t_0}^{t_f} \frac{1}{f_1(t)} \left\{ \left(\frac{3V}{4\pi W} \right)^2 + \frac{1}{2a} \ln \frac{1+\alpha}{1-\alpha} + W \right\} dt \right] \quad (2.25)$$

where
$$\alpha = \frac{W - (3V/4\pi W)^2}{W} \quad (2.26)$$

$$W = (a_0 + a_p / \sin 0.5Wt)^2 \quad (2.27)$$

$$f_1(t) = \frac{(a_0 2b - (a - x_0)^2 (b_0 - x_0)) - 2abx_0 + bx_0^2}{a^2 - 2ax_0 + x_0^2} = X \quad (2.28)$$

$$a = a_0 + a_p |\sin 0.5wt| \quad (2.29)$$

and

$$b = \frac{3V}{4\pi a^2} \quad (2.30)$$

A correlation to estimate the frequency of oscillation was proposed by Schroeder and Kintner(1956) gives

$$w^2 = \frac{\alpha b_1}{r^3} \frac{n(n+1)(n-1)(n+2)}{[(n+1)\rho_d + n\rho_c]} \quad (2.31)$$

where
$$b_1 = \frac{d_{3e}^{0.225}}{1.242} \quad (2.32)$$

and n is the mode of oscillation, when n = 0,1 correspond to rigid body motion. The fundamental mode correspond to n = 2:

$$K_d = 0.45(D_d w)^{0.5} \quad (2.33)$$

Anglo et al (1966) also based their model on surface stretch and internal mixing of the drop. They expressed the periodic change of the surface area for an oscillating droplet as:

$$A = A_0(1 + \varepsilon \sin^2 wt) \quad (2.34)$$

where

$$\varepsilon = \frac{A_{\max}}{A_0} - 1 \quad (2.35)$$

Equation 2.20 allows an analytical integration of the resulting mass transfer relations and yields the following relation for the mass transfer coefficient

$$K_d = \left[\frac{4D_{dv}(1 + \varepsilon_0)}{\pi} \right]^{\frac{1}{2}} \quad (2.36)$$

$$\text{where } \varepsilon_0 = \varepsilon + \frac{3}{8}\varepsilon^2 \quad (2.37)$$

Another model for oscillating droplets was proposed by Ellis(1966) which is based on the assumption that oscillating droplets could be divided into different regions of mass transfer. This division of the droplet is not in agreement with the physical phenomena of drop oscillation and also the shape of the drop is not a sphere during oscillation Alhassan (1979).

2.10 Mass Transfer in the Continuous Phase

The overall mass transfer process between dispersed and continuous phase, includes the contribution of mass transfer in the continuous phase. This is very difficult to estimate due to the wake of the drop. Thus the process usually described as an overall process for the whole drop, using the continuous mass transfer coefficient. This coefficient may be evaluated in terms of the resistance in the film surrounding the drop through which the transfer takes place by molecular diffusion and mass transfer coefficient becomes

$$K_c = \frac{D_c}{X_c} \quad (2.38)$$

where X_c is a continuous phase fictitious film thickness. A great number of investigations have been done to derive a theoretical or empirical

correlation for the continuous phase mass transfer coefficient. Summaries of these investigations can be found in the work of Linton et al (1960), Sideman et al(1964) and Griffith(1960).

The internal droplet circulation has an important effects on the outside mass transfer coefficient K_c . The different mechanisms of mass transfer in the continuous phase from or to a droplet, dependent on the hydrodynamics state of the droplets are therefore considered below.

2.10.1 Mass transfer From and to Stagnant Droplets

For the case of a rigid drop theoretical analysis by Garner and Suckling (1958) based on the boundary layer theory, have shown that the rate of mass transfer from or to a solid sphere can be correlated by a general equation of the form

$$Sh = A + C Re^m Sc^n \quad (2.39)$$

where A, C, m and n are constants.

Examples from the literature are compiled in Table (2.2) Equation (2.25) has been proposed by Linton et al (1960) and recommended by Griffiths (1960). However, in a study by Rose et al(1965) Equation 2.24 was proposed which included a term accounting for the diffusion process.

2.10.2 Mass transfer From and to Circulating Droplets

Many studies Garner et al (1960) have indicated that the continuous phase mass transfer coefficient is increased when circulation occurs inside a droplet and this is explained by the reduction in the boundary layer thickness. The correlations proposed to describe the mass transfer coefficient of the continuous phase surrounding a circulating droplet are similar to those given for stagnant drops, i.e., K_c found via a Sherwood number relation. These correlations are given in Table (2.4).

In a previous study by Mekasut et al(1978) on the transfer of iodine from aqueous continuous phase to carbon tetrachloride drops the resistance to mass transfer was assumed to be solely in the continuous phase. The

Sherwood number was correlated with the Galileo number ($Ga = D^3 \rho_c^2 g / \mu_c^2$) in Equation 7 for drops of less than 0.26 cm in diameter.

Table 2.4 Correlation for Continuous Phase Mass Transfer Coefficient

Authors and References	Correlation	Equation No.	State of Drops	Comment
Linton and Sutherland	$Sh_c = 0.0583(Re)^{0.5}(Sc)^{0.33}$	1	Stagnant	Ignore diffusion and wake effect
Rowe et al	$Sh_c = 2 + 0.076(Re)^{0.5}(Sc)^{0.33}$	2	Stagnant	Account for diffusion Process
Kinard et al	$Sh_c = 2 + (Sh_c) + 0.45(Re)^{0.5}(Sc)^{0.33}$	3	Stagnant	Include diffusion process and wake effect
Boussinesq	$Sh_c = 1.13(Re)^{0.5}(Sc)^{0.5}$	4	Circulating	Claimed to be valid for many systems
Garner and Tayeban	$Sh_c = 0.6(Re)^{0.5}(Sc)^{0.5}$	5	Circulating	Inapplicable to $Re > 450$
Garner et al	$Sh_c = 126 + 1.8(Re)^{0.5}(Sc)^{0.42}$	6	Circulating	For partially miscible binary system of low interfacial tensions
Mekaut et al	$Sh_c = 1.04(Ga)^{0.49}$	7	Circulating	Ga is Galileo number
Garner and Tayeban	$Sh_c = 50 + 0.085(Re)(Sc)^{0.7}$	8	Oscillating	Successfully used by Thorsen et al (156)
Yamaguchi et al	$Sh_c = 1.4(Re)^{0.5}(Sc)^{0.5}$	9	Oscillating	
Mekasut et al	$Sh_c = 6.74(Ga)^{0.34}$	10	Oscillating	Ignore the effect of infrequency of oscillation

2.10.3 Mass transfer From and to Oscillating Droplets

Many workers Skelland, et al (1971) have used correlations to estimate mass transfer rates for oscillating drops with turbulent internal circulation, but the effect of oscillation causes higher rates of mass transfer than circulation Rose et al(1966). Garner and Tayeban (1960) proposed the most acceptable correlation to predict the mass transfer coefficient of continuous phase surrounding an oscillating droplet. They reported a Schmidt number exponent more than 0.5 because, for oscillating drops, there is less dependence on diffusivity Alhassan (1971), Yamaguchi et al (1975) proposed Equation 9 in table 2.2 with a modified Reynolds number ($Re = \rho_c d c^2 / \mu c$) for oscillating drops, which neglects the drop velocity. They reported that the maximum deviation of the data from that predicted is approximately $\pm 20\%$. Finally another approach was used by Mekasut et al(1978) who correlated the Sherwood number with the Galileo number in Equation 10 to predict the mass transfer coefficient of the continuous phase for oscillating drops. They ignored the effect of the frequency of the oscillating drop.

2.11 Mass Transfer During Coalescence

Mass transfer in a coalescing environment is a rather complex process, numerous studies have been made of coalescence mechanisms, but there is little information as to the effects of mass transfer on coalescence and vice versa. Many investigators have found that coalescence rates are greatly affected by the presence of mass transfer. The rates were also dependent on the direction of transfer. Groothuis and Zwiderweg (1960) observed that this was only applicable if the solute decreases the interfacial tension. McFerrin and Davidson(1971) using the system water-di-isopropylamine-salt, in which the solute salt increased the interfacial tension, found that the transfer into the drop

aided coalescence and out of the drop hindered it. Heertjes and de Nie (1971) concluded that the effect of mass transfer on the rate of coalescence of drops in binary systems could not be entirely explained by interfacial phenomena alone as suggested by previous workers.

Little information is available on the effect of coalescence on mass transfer. Johnson and Hamielec (1960) proposed a highly simplified expression for K_{dc} for a drop coalescing immediately upon reaching the phase boundary. Mass transfer was regarded as occurring according to the penetration theory and the time of exposure of the layer was taken to be the same as the time of drop formation thus:

$$K_{dc} = \left(\frac{D_d}{\pi t_f} \right)^{0.5} \quad (2.40)$$

Similar results were reported by Licht and Conway (1950) and Coulson and Skinner (1951) but, Skelland and Minhas (1971) subsequently criticised the above models and concluded logically that the amount of mass transfer during coalescence is insignificant compared to that during drop formation. Therefore for all practical purposes transfer during coalescence might be ignored, though they correlated their experimental results for mass transfer coefficient during drop coalescence as

$$\frac{K_{dc} t_f}{d} = 0.1727 \left(\frac{\mu_d}{\rho_d D_d} \right)^{-1.115} \left(\frac{\Delta \rho g d^2}{c} \right)^{1.302} \left(\frac{V_t^2 t_f}{D_d} \right)^{0.146} \quad (241)$$

The average absolute deviation from the data was around 25%. The insignificant mass transfer during drop coalescence has been confirmed by Heertjes and de Nie (1971) who argued that drainage of drop-contents in a homophase. Further, since coalescence on impact with an interface is almost instantaneous (of the order of 3×10^{-2} sec), very little mass transfer is expected. This is particularly true in the case of agitated columns where efficient mass transfer occurs in the column. Reference

here is only made to the coalescence of drops at an interface and substantial work has been performed with regard to mass transfer during interdroplet coalescence. However, generally the coalescence of drops in swarms causes an increase in drop size, and thus oscillation, and a decrease in surface area. These factors counteract each other with respect to mass transfer rate.

2.12 Overall Mass Transfer Coefficients

The overall mass transfer coefficient is the sum of the individual phases mass transfer coefficient. The resistance to mass transfer in one of the phases is often predominant, and design can then be based on that phase. The determination of which phase is controlling the mass transfer requires the knowledge of the time for a droplet to attain 60% or 90% solute concentration. The phase requiring the larger time is controlling the mass transfer. The time t , may be estimated from the following equations Mumford (1970). For the dispersed phase

$$\frac{Q_t}{Q_0} = 1 - \exp\left[-2.25\left(\frac{4D_d\pi^2t}{d^2}\right)\right] \quad (2.42)$$

and for the continuous phase

$$\frac{Q_t}{Q_0} = 1 - \operatorname{erf}\left[\frac{X}{\sqrt{4D_c t}}\right] \quad (2.43)$$

erf : error function.

2.13 Application of Single Drop Mass Transfer Models to Agitated Extraction Columns

Although studies of mass transfer in agitated contractors are an extension of single drop behaviour to swarms, the direct application of single drop data is of limited value, because of the complex interaction

between drops of different sizes in a swarm. The basic differences may be summarised as:

In the case of single drop mass transfer, the driving force may be evaluated to a reasonable degree of accuracy. Difficulties arise in the estimation for an agitated column owing to axial mixing.

Mass transfer coefficient predicted from a single drop model are usually considerably lower than values obtained in agitated systems. This is due to the phenomena of coalescence-redispersion and associated surface renewal effects which predominate in an agitated contractors.

Drop break-up may lead to a higher surface area but a lower mean mass transfer coefficient due to the change in mode of mass transfer.

A wide range of drop sizes exists in the column giving rise to different modes of mass transfer and also a residence time distribution.

Application of single drop mass transfer models become doubtful to design an industrial agitated contractor, due to different in hydrodynamic of single and swarm of droplet.

Most of mass transfer correlations presented in table (2.3) and (2.4) apply to pure systems with the minimum of impurities under ideal conditions, and these seldom exist in practice.

2.14 Mass Transfer and Interfacial Instability

Various types of ancillary flows generated at the interface and in the layers immediately adjacent to it are usually classified as interfacial turbulence. Such turbulence induces a substantial increase in the rate of mass transfer between the two phases. Thus transfer rates may be much

higher than predicted from a proper combination of single-phase rate coefficients on the assumption of a quiescent interface.

Sterling and Scriven (1959) in their analysis of this phenomena, suggested that interfacial turbulence is usually promoted by:

1. Solute transfer out of the phase of higher velocity;
2. Solute transfer out of the phase in which its diffusivity is lower;
3. Large differences in kinematics viscosity and solute diffusivities between the two phases;
4. Steep concentration gradients near the interfaces;
5. Interracial tension that is highly sensitive to solute concentration;
6. Absence of surface active agents.

Sterling and Scriven (1959) showed that some systems may be stable with solute transfer in one direction yet unstable with transfer in the opposite direction. Orell and Westwater (1962) have confirmed some of the above conditions. Maroudas and Sawistowski (1965) in their study on the simultaneous transfer of two solutes across liquid-liquid interface found that both solutes produced spontaneous interfacial disturbances, termed 'eruptions', during mass transfer in either direction. This is contrary to the stability criteria of Sternling and Scriven (1959). Mass transfer in the eruptive regime, however, cannot be explained by penetration and surface renewal theories Sarkar (1976).

Sehrt and Lande (1967) observed that the presence of spontaneous interfacial convection in rising and falling drops will affect the drag coefficient in addition to the rate of mass transfer. This is due to reduction the extent of internal circulation in the drop and thus increases the form drag.

Haydon's (1958) developed a theory implying that spontaneous interfacial turbulence should occur with transfer of solute in either direction. Maroudas and Sawistowski (1965) found their experimental

results agreed with Haydon's theory. And hence concluded that Sterling and Scriven theory is too simple to give a reliable criterion of interfacial instability. Finally Davies (1972) reported an interesting quantitative result for the extraction of acetic acid from benzene drops rising through water, that the rate of mass transfer of acetic acid is higher by a factor of 5.9, if 5% butanol is initially present in the benzene. Butanol causes spontaneous interfacial turbulence which accelerates the transfer of acetic acid. With 10% of butanol in benzene, the acetic acid transfer is 8.8 times higher than without the butanol West et al(1952).

2.15 Effect of Surface Active Agent

A trace amount of surface-active substances, unknown in structure and concentration, are frequently present in commercial equipment. This leads to difficulties in interpreting the performance of plant in terms of experimental and theoretical studies of mass transfer. These surface-active materials can be surfactant, impurities or metallic colloids from pipe fittings. The presence of a surface layer of a surface-active material, has a significant effect on the rate of mass transfer and interfacial tension. This is due to the introduction of a surface resistance to diffusion across the interface. The reduction in mass transfer rate can be large and this will introduce an additional resistance into the "resistance-additivity" equation. Thus reduction in interfacial tension will become less dependent on solute concentration and the interface compressibility will also decrease, thus adversely affecting surface renewal Sawistkewski (1971). In addition surface viscosity will increase and tends to slow down any movements in the surface. It has been demonstrated that surface active materials make droplets more rigid and cause the mass transfer rates to approach that of stagnant droplet Garner et al (1965). This is because the droplet internal circulation is reduced due to the

presence of the surface active materials which will sweep back towards the rear of the moving drop. Garner and Hale (1965) showed that the addition of small quantity of teepol (0.015% by volume) to water reduce the rate of extraction of diethylamine from toluene drops to 45% of its original value. An even greater reduction (68%) has been reported by Lindland and Terjesen (1956) and about 70% by Holm and Terjesen (1955) using a stirred liquid-liquid extractor. Hung and Kintner(1976) in their study of mass transfer characteristics, showed that the surface film reduces both the extent of internal circulation and also the area of the interface being renewed. The mass transfer rate to or from oscillating drops is also affected by traces of surface-active materials. This may be due to surface tension gradients and the rigidity of the surface inhibiting the surface movement of the drop as it oscillates Davies et al(1972). Never the less, in this work surfactants are used to make stable emulsion of oil in water, which makes solute (oil) partially miscible with the water.

2.16.1 Mass Transfer Models

The simplest mass transfer model is that which neglects axial mixing and assumes piston flow of the phases through the column. This situation is shown diagrammatically in figure 2.2

H_c , X_R and Q_R are the solute concentration and the flowrate of the raffinate phase

$$(N.T.U.)_{O.R} = \int_{X_{R2}}^{X_{R1}} \frac{dX_R}{(1-X_R) \ln \frac{(1-X_R)}{(1-X_R)}} = \frac{H_c}{(H.T.U.)_{O.R}} \quad (2.44)$$

$$(N.T.U.)_{O.R} = \frac{Q_R}{K_R a (1-X_R)_{o.m} C_{R.av}} \quad (2.45)$$

where

$$(1-X_R)_{o.m} = \frac{(1-X_R) - (1-X_R)}{\ln \frac{1-X_R}{1-X_R}} \quad (2.46)$$

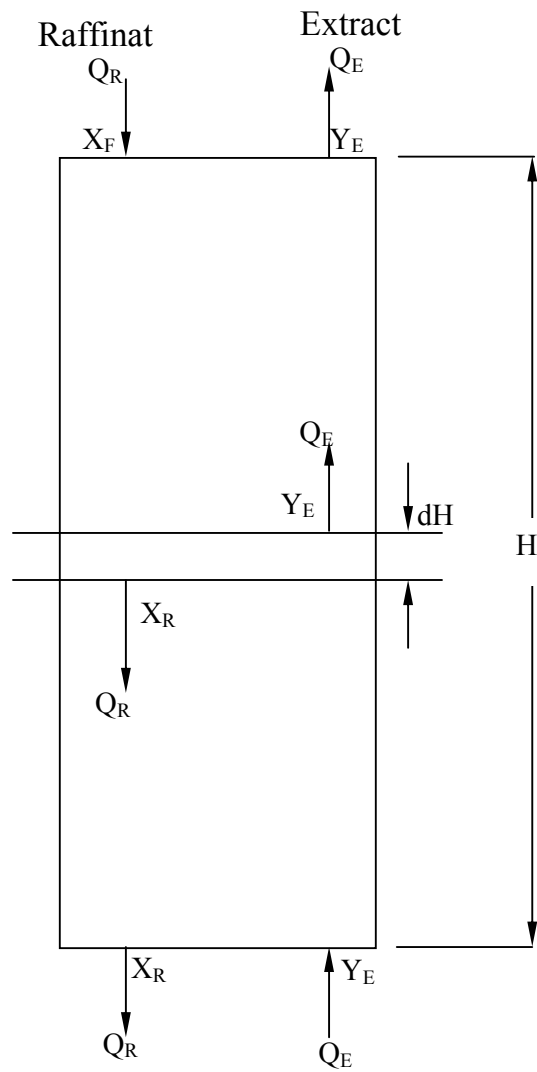


Fig. (2.2): Piston flow model

and

$$C_{R,av} = \frac{C_{RM1} + C_{RM2}}{2} \quad (2.47)$$

where C refers to total concentration of all substances present in the raffinate phase.

Better prediction of mass transfer efficiency has been shown to be possible by including the effect of the axial mixing in the process of the mass transfer modelling. Four such models are discussed below.

2.16.2 Stage Model

This is the simplest model to describe mass transfer with longitudinal mixing in counter-current extraction columns Young (1957). A diagrammatic representation of the model is shown in figure 2.3

In this model each stage is assumed to be perfectly mixed so that the solute concentrations in streams leaving any stage are identical with those in the same phase throughout the stage. Axial mixing is only recommended for cases where the extent of the axial mixing in both phases is similar and where its influence on the mass transfer is not high. Miyauchi et al(1963) considered that the model could only be used when:

- a) Interdroplet coalescence is frequent, or
- b) The drop size distribution would narrow the distribution coefficient m, hold-up, x and mass transfer coefficient k.

A material balance on ith stage is described by

$$Q_R(X_i - X_{i-1}) = Q_E(Y_{i+1} - Y_i) \quad (2.48)$$

and the mass transfer in the ith stage by

$$X_i - X_{i-1} = \frac{K_x all}{Q_R} (X_i - X_i^*) \quad (2.49)$$

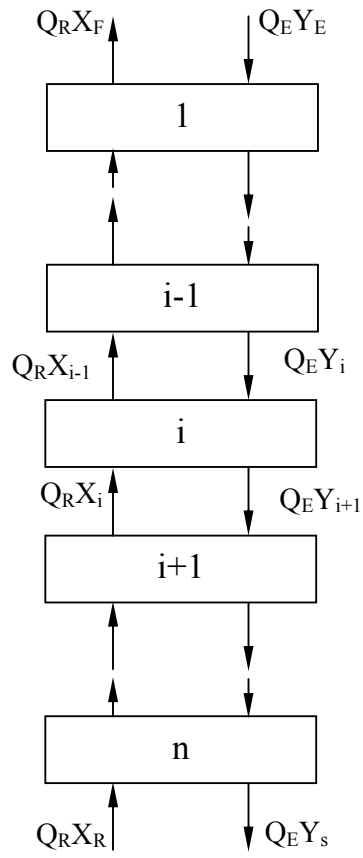


Fig. (2.3): Stage flow model.

The boundary conditions are

$$\begin{array}{ll} X_0 = X_F & Y = Y_E \\ X_n = X_R & Y_{n+1} = Y_s \end{array}$$

Analytical solution is required for Equations (2.46) and (2.48) for the linear case, and graphical solution required for the non-linear case Sicicher(1959).

2.17 behaviour of drops in oil-water Emulsion

The behaviour of drops of oil as dispersed phase and water as a continuous phase was investigated by Sajjadi (2000). Sajjadi observed that. The size of internal oil droplets continuously decreased with time until it reached a steady-state value., the size of multiple water drops either reached a steady-state value or continued enlarging until equilibrium He observed that by reducing the surfactant concentration, the ability of the dispersed phase to entrain the continuous phase decreased so that no minimum was achieved for the size of multiple drops with time, similar to conventional systems with simple drops. The size distribution of the multiple water drops initially narrowed and then widened again, whereas the size distribution of internal oil droplets continuously narrowed with time until it reached a constant value. The possible mechanisms for complex drop formation were discussed and drop deformation was suggested as the main cause for inclusion of a low dispersed phase ratio Sajjadi (2000).

It was observed that the drop breakage rate dominates the drop coalescence rate in the initial stage of stirring, which causes the drop sizes to decrease with time , Arishman, et al (1980) .As stirring proceeds, the drop breakage rate decreases while drop coalescence rate increases. hence, a steady state is reached where the rate of both processes become

equal, and a steady-state drop size distribution is established. Hong and Lee(1983) indicated that the average drop size during the initial period of mixing decreases exponentially while the size distribution changes less drastically from wide to narrow. The effects of dispersed phase volume fraction and surfactant concentration need to be studied and analyzed.

2.17.1 Analysis of drop

The drop diameter, the Sauter diameter and polydispersity index (PDI), were calculated by the following equations:

$$d_n = \sum n_i d_i / \sum n_i \quad (2.50)$$

$$d_s = d_{32} = \sum n_i d_i^3 / \sum n_i d_i^2 \quad (2.51)$$

$$d_{32} = \sum n_i d_i^4 / \sum n_i d_i^3 \quad (2.52)$$

$$PDI = d_w / d_n \quad (2.53)$$

Where n_i is the number of drops with diameter d_i , d_s is equivalent Sauter mean diameter, d_{32} , generally used to analyze liquid-liquid dispersion systems.

2.17.2 Drop size measurement

The side of drops were measured by normal method of video camera by sizing the drops from enlarge photos.

The procedure stated in details by sajjadi (2000).

2.18 Equipment Classification

There are two major categories of equipments for liquid extraction.

- (A) Stagewise Contactors, in which liquids are mixed, extracted and separated in discrete stages. This class includes the mixer settler range of equipment.
- (B) Differential Contactors, in which continuous counter-current contact is established between the immiscible phase to give the

equivalent of any desired number of stages. These may be categorised as

- (1) Gravity Operated Extractors
 - (a) Non-mechanical dispersion
 - (I) Baffle Plate Columns
 - (II) Spray columns
 - (III) Packed columns
 - (IV) Perforated-plate columns
 - (b) Mechanically Agitated columns
 - (I) Pulsed columns
 - (II) Rotary Agitated Columns
 - (i) The Rotating Disc Contactor
 - (ii) The Schiebel Column
 - (iii) The Oldshue-Rushton Column
 - (iv) The Assymetric Rotating Disc Contactor

A summary of the agitated column design is given in Table (2.5)

2.19 Selection of Equipment

Continuous contactors are generally preferable to mixer settlers when large throughputs are to be handled since they offer economies in agitation and power cost, floor space and solvent inventory. They operate with relatively small amounts of hold-up of raffinate and extract. This is important when processing radioactive flammable, expensive or low stability materials. In extraction processes it is necessary as a final step, or in multi-contact stagewise equipment, at intermediate steps, to separate the two phases. Rapid coalescence is desirable otherwise an excessive residence time is required or some of the continuous phase will be removed with the 'bulk' dispersed phase, resulting in reduced efficiencies, capacity and loss of solvent. Hence the contractor which gives the most rapid solute transfer is not necessarily the most economic.

Continuous columns without mechanical agitation are unsuitable for use with systems of high interfacial tension since adequate dispersions cannot be achieved throughout continuous phase. Centrifugal extractors have relatively high capital and operating costs and the number of stages which can be accommodated in a single unit is limited. Nevertheless they are superior to all other contactors for processes requiring a low hold-up or low contact time, or if there is a low density difference between the phases Khandel wal(1978).

Table 2.5 Continuous Differential Contactors. Gurashi (1985)

Contactors	Type	Comment
1. RDC	Contrally located discs driven in compartments separated by stator rings by a central shaft.	Operation reasonably flexible: efficiency not much affected by phase flow ratio: H.E.T.S. is remarkably low, around 20 per cent of that for a simple packed tower. Hydrodynamics and mass transfer characteristics are partially known.
2. A. R. D. C.	Similar to the R. D. C. except that the rotor is off-set from the column axis; separations of phases take place in a shielded transfer section.	Fixing and separation zones claimed to reduce backmixing; but phase entrainment does occur in settling zone reducing overall efficiency. No special advantages over R.D.C.
3. Oldshue Rushton	Vertical column divided into compartments by horizontal stator rings with vertical baffles in each compartment. Turbine in each compartment driven by a central shaft.	Coalescence-redispersion is predominant. Stage efficiencies obtained by Oldshue and Rushton varied from 40 to 90%. H.E.T.S. was nearly half that of a simple packed tower of same diameter.
4. Ziel Extractor	Vertical column terminating at top and bottom in large vessel to assist settling. The stirring mechanism consists of a shaft fitted with a number of star-shaped impellers. Vertical, reciprocal, as well as rotary motion is imposed on the impellers for effective mixing.	Theoretical efficiencies claimed to have been attained in the manufacture of phenol formaldehyde resin. No mass transfer data is available.

Table (Continued)

Contactor	Type	Comment
5. Scheibel Column	Consists of alternate fully-baffled mixing sections and packed sections. Agitation is provided by centrally located impellers.	Coalescence-redispersion is predominant. Mass transfer coefficient is related by $Ka = c \left(\frac{\nabla e}{\gamma} \right)^{1.5}$ Capacity is limited by permissible flow rate through the packing.
6. Khuni Extractor	Incorporates the principles of R.D.C. Oldshue-Rushton and sieve plate columns. Divided into compartments by plates perforated only at the centre so that flow from one compartment to the next is directed towards the agitator. Each compartment has four vertical baffles. Impeller agitator for effective settling.	Published mass transfer data are limited. Capacity and scale-up are expressed by $\frac{d}{D} = C.Re^{0.61}.we^{0.6}.Fr^{0.05}$ The design allows for only low through-puts. Modified designs have found limited application.
7. Pulsed Columns	Phases are interdispersed by inducing a pulsating motion either by means of diaphragm pump or a valveless piston. A variety of internal packing or baffles may be used. In one design the plates are pulsed	Commercial application is limited. Employed in the extraction of metals from radioactive solutions. Power requirements are high. No published information is available for scale-up. Mass transfer data have been reported by various authors.

Table (2.6) Advantages and Disadvantages of Various Contractors. Logsadil (1971)

Type	Capital Cost	Operating and Maintenance Costs	Efficiency	Total Capacity	Flexibility	Volumetric Efficiency	Space		Ability to Handle Systems that Emulsify
							Vertical	Floor	
Spray Tower	5	5	1	2	2	1	0	5	3
Baffle Plate Tower	4	5	2	1	2	3	1	5	3
Packed Tower	4	5	2	2	2	2	1	5	3
R.D.C.	3	4	4	3	5	4	3	5	3
Pulsed Plate Column	3	3	4	3	4	4	3	5	1
Mixer settler	2	2	3	4	3	3	5	1	0
Centrifugal	1	2	5	3	5	5	5	5	5

0 = Unsuitable, 1 = poor, 2 = Fair, 3 = Adequate, 4 = Good, 5 = Outstanding (preferred)

Table (2.6) is a useful ‘rule of thumb’ method for a preliminary narrowing of the choice between the various types of extractor (Todd 1957). Special process factors often govern extractor selection. Equipment installation and operating costs are of primary importance. On this basis, and dependent on the number of stages for a given application and the case of phase dispersion/separation, an extractor selection chart can be drawn for any given feed rate range.

In general the choice of equipment for a given separation should be based on the minimum annual cost for the complete plant, i.e., extractor and ancillary equipment, as well as an operating and solvent loss costs.

Previously Logsdail (1971) has described the various design considerations and process parameters to be considered in arriving at a decision on solvent extraction equipment. The various factors and choice of extractors are outlined in table (2.6).

2.20.1 Phase Equilibrium

In liquid extraction, the phase equilibrium of interest are those showing the distribution of the solute(c) between the two immiscible or partially miscible liquids (A) and (S). in the case where the natural solubility of liquids (A) and (S), even in the presence of the solute (C), is negligible [immiscible liquids], the equilibrium becomes a simple relation between the concentrations of the solute (C) in the two phases. The equilibrium condition, is conveniently considered in terms of the distribution law. Thus, at equilibrium:

The ratio of the concentrations of the solute in the two phases is given by:

$$K = \frac{x_{cs}}{x_{ca}} \quad (2.54)$$

Where K - distribution coefficient.

The equilibrium relation is easily shown by a plot of the concentration of the solute in one phase against the concentration in the other phase.

But, when the mutual solubility of the carrier (A) and solvent (S) cannot be neglected; [partially miscible liquids]; the solubility and equilibrium diagram, the limits of mutual solubility are marked by the bimodal curve and the compositions of phases in equilibrium by tie lines. The region within the dome is two phase and that outside is one phase. The miscibility boundary (saturation curve) can be obtained experimentally by a cloud point titration. To obtain data to construct tie lines, it is necessary to make a mixture (A, C, S), equilibrate it, and then chemically analyze the resulting extract and raffinate phases. At the plait point, the two liquid phases have identical composition. Each corner of the triangular diagram represents a pure component.

This case is the most commonly encountered, and a number of phase diagrams and computational techniques have been devised to determine the equilibrium compositions. The graphical methods are still used to represent equilibrium data and perform extraction calculations for ternary systems. However, these methods are tedious and can't be used directly in cases requiring computer analysis. Hence, methods for prediction of phase equilibrium and correlation of tie line data have been developed.

2.20.2 Tie-line Correlations

In the case of many systems described in the literature, only a few tie lines have been experimentally determined. Direct interpolation of such data may lead to highly inaccurate results. Several tie line correlations in equation four have been proposed (identified with these subscripts):

CA = solute C in carrier phase A.

AA = carrier A in carrier phase A.

SA = solvent S in carrier phase A.

CS = solute C in solvent phase S.

AS = carrier A in solvent phase S.

SS = solvent S in solvent phase S.

2.20.3 Othmer and Tobias' Correlation

Othmer and Tobias have found that a plot of conjugate values of $\frac{1-x_{AA}}{x_{AA}}$ against $\frac{1-x_{SS}}{x_{SS}}$ on logarithmic coordinates produced straight lines useful for interpolation and extrapolation Othmer, etal (1942):

$$\frac{1-x_{SS}}{x_{SS}} = K \left(\frac{1-x_{AA}}{x_{AA}} \right)^n \quad (2.55)$$

These methods suffer from the fact that the concentration of the distributed component (C) is not indicated in the coordinates.

2.20.4 Hand's Correlation

Hand showed that a logarithmic plot of $\frac{x_{CA}}{x_{AA}}$ against $\frac{x_{CS}}{x_{SS}}$ (which includes the concentration of the distributed component (C) in the coordinates), gives generally a rectilinear plot. Hand's equation for the correlation of tie-line data is ,Hand (1930),:

$$\frac{x_{CS}}{x_{SS}} = K \left(\frac{x_{CA}}{x_{AA}} \right)^n \quad (2.56)$$

Furthermore, a simple method for estimating the entire equilibrium diagram and locating the plait point based on this method has been devised. If on the same graph as the tie-line data the bimodal curve is plotted as $\frac{x_C}{x_S}$ against $\frac{x_C}{x_A}$, where x_A , x_C , and x_S are concentrations of the components at any point on the bimodal curve, a single curve of two

branches is obtained, one branch representing the A-rich layer and the other the S-rich layer.

At the plait point, the distinction between the A-rich and the S-rich phases disappears:

$$\left[\left(\frac{X_{CS}}{X_{SS}} \right)_P = \left(\frac{X_{CA}}{X_{SA}} \right)_P = \left(\frac{X_C}{X_S} \right)_P \right] \text{ and } \left[\left(\frac{X_{CA}}{X_{AA}} \right)_P = \left(\frac{X_{CS}}{X_{AS}} \right)_P = \left(\frac{X_C}{X_A} \right)_P \right] \quad (2.57)$$

When subscript P represents the plait point. Since the plait point represents a limiting line, the coordinates $\left(\frac{X_{CA}}{X_{AA}} \right)_P$ and $\left(\frac{X_{CS}}{X_{SS}} \right)_P$ must fall simultaneously on the tie line correlation and on the bimodal curve. Extrapolating the straight line tie-line correlation to intersect with the solubility curve will locate the plait point.

2.20.5 Ishida's correlation:

Ishida's equation for the correlation of tie-line data is:

$$\frac{X_{SA}X_{CS}}{X_{CA}X_{SS}} = K \left(\frac{X_{AS}X_{SA}}{X_{AA}X_{SS}} \right)^n \quad (2.58)$$

Where K and n are constants. This equation should plot linearly on logarithmic coordinates, Rod,(1966).

CHAPTER THREE

MATERIALS AND METHODS

3.1 Selection of Liquid-Liquid Chemical Systems

The system used in this work was oil –water-n.hexane which was selected due to the following reasons:

1. Oil in water makes a serious pollution problem in the premises of oil fields and refineries in Sudan.
2. the two solvents i.e., water and n-hexane are almost completely immiscible.
3. the physical properties of the two systems such as density surface tension, specific gravity, and viscosity are different.
4. the system is industrially and environmentally important.
5. the analysis of the liquid mixtures can be performed on various devices such as liquid chromatographs, refractometers, and electro-photometers.
6. the solute has a high selectivity in normal hexane.
7. equilibrium data could be obtained through experiments with Smith-Bonner cell.

3.2 Sampling Procedures

Waste water samples were taken from main discharge channel which leads the final waste water from Abugabra filed to the open area .The sample of waste water were collected in 36 liters capacity plastic containers .

The physical and chemical properties of n. hexane and waste water were shown in appendix 2

3.3 Description of Equipment

The unit is a sieve tray column of 110cms in lengths ,30cms in diameter and has 10 trays it was situated in the unit operation pilot plant in Gezera University.

The body is provided with 9 stages. Each of which has a tray space. An agitator shaft with blades is vertically arranged in the center of column.

Heavy liquid and light liquid are supplied into the column interior from the column top and bottom respectively by means of piston pumps. These liquids make contact with each other inside the column .mean while, the oil –water emulsion are mixed to small drops in each stage with the solvent through agitation. Thus permitting perfect mixing and better contact of the phases.

Volume of each feed liquid was controlled by adjusting the dial of each pump. And The number of revolutions of the agitator shaft can be controlled by manual adjustment

For the function of each section of the unit and the overall assembled condition, see Figure.(3.1). This would Provide about 10 liters of fresh water in each tank to start test operation. Each pump shall be Operated each pump to feed the fresh water into the system, check if no leak of water takes place.

In case a leakage is observed, necessary countermeasures should be taken. In most cases this problem can be solved by further fastening of the piping and joints.

Operate the D.C. motor, increase the dial readings of revolving controller gradually, starting from (0). In this case, take good care not to operate the motor at a high rotating speed.

The fresh water thus fed into the system should be drained out. It takes approximately an hour for complete drainage.

The capacity of each tank is 25 liters.

3.3. 1 Determination of flooding points:

Flooding is brought by excessive flow, causing liquid to be entrained in vapour.

This is carried out without mass transfer

Procedure:

The column was filled with the continuous phase and flow rate was adjusted, and agitation was started at low speed of agitation (200 rpm).then, this is followed by:

Introducing the dispersed phase at low flow rate and continuously increasing until flooding. Repeat 2 through 3 at different agitator speed (200,300,500,and 600 rpm).

Increase the flow rate of the continuous phase, and repeat 2 through 4

The result is shown in figure (4.1) and table (4.1)



Fig. 3.1 Photo pilot plant sieve tray column

3.4 Experimentation

Experiments to determine the transfer of oil from the aqueous emulsion phase to n-hexane phase were performed, and phase's flow rates were kept below 85% of flooding flow rates under non-mass transfer conditions.

The procedure followed during these operations was: Before starting experiments n-hexane was mutually saturated by circulating it in closed loop for approximately 6 hours afterwards it was left overnight to settle and separate, the column was then filled with the continuous phase (oil-water emulsion), the agitator adjusted to the required speed.

The dispersed phase n-hexane was introduced into the column and its flow rate adjusted. The continuous phase was introduced into the column and its flow rate adjusted to the required level.

After steady-state condition has been reached, about 20minutes samples and photographs were taken for analysis. The same was repeated at different flow rates at various solvent to liquid ratio, with and without mass transfer, the speed of agitation was also varied.

3.5Determination of Equilibrium

Equilibrium concentrations were determined by making up mixtures on weight basis to represent points below the solubility curve.

Each mixture was contained in Smith-Bonner cell and brought to equilibrium through agitation and standing for several hours. The layers were then separated using separating funnel and sample were analyzed using the electro photometer.

Determination of Sauter mean diameter: Digital camera was employed for this photography. Three photographs were taken for each events and then used a hand lens (x4) and venire caliper to count the

number of drops and the diameter of each drop was determined. Result shown in tables (4.2) up to (4.17)

3.6 Calculation Method

3.6.1 Experimental mass transfer coefficient

The over all experimental dispersed phase mass transfer coefficient under each set of operating conditions was calculated using

$$N = KA(\Delta C_m) \quad (3.1)$$

where N is the mass transfer rate

$$A = a * V \quad (3.2)$$

$$a = \frac{6x}{d_{32}} \quad (3.3)$$

where a is specific interfacial area in cm² per cm³ of the column volume, and v is the column volume. Simpson rule was applied to determine the actual mean driving force (ΔC_m) by using the oil concentration profile a long the column. Oil concentration was determined in samples of continuous phase taken from trays number 1,2,3 up to 7, the driving force in these trays can be determine as Δy_1 , Δy_2 , Δy_3 and Δy_7 respectively, where

$$\Delta y = y^* - y \quad (3.4)$$

and y is the oil concentration of aqueous phase so Simpson's rule is:

$$\Delta y_m = \frac{1}{18} \{ \Delta y_{top} + \Delta y_{bot} + 4(\Delta y_2 + \Delta y_4 + \Delta y_6) + 2(\Delta y_3 + \Delta y_5) \} \quad (3.5)$$

Δy_m was then converted to ΔC_m by dividing it by the extract phase density, so the over all experimental mass transfer coefficient can be calculated as

$$K_{exp} = \frac{N}{A\Delta C_m} \quad (3.6)$$

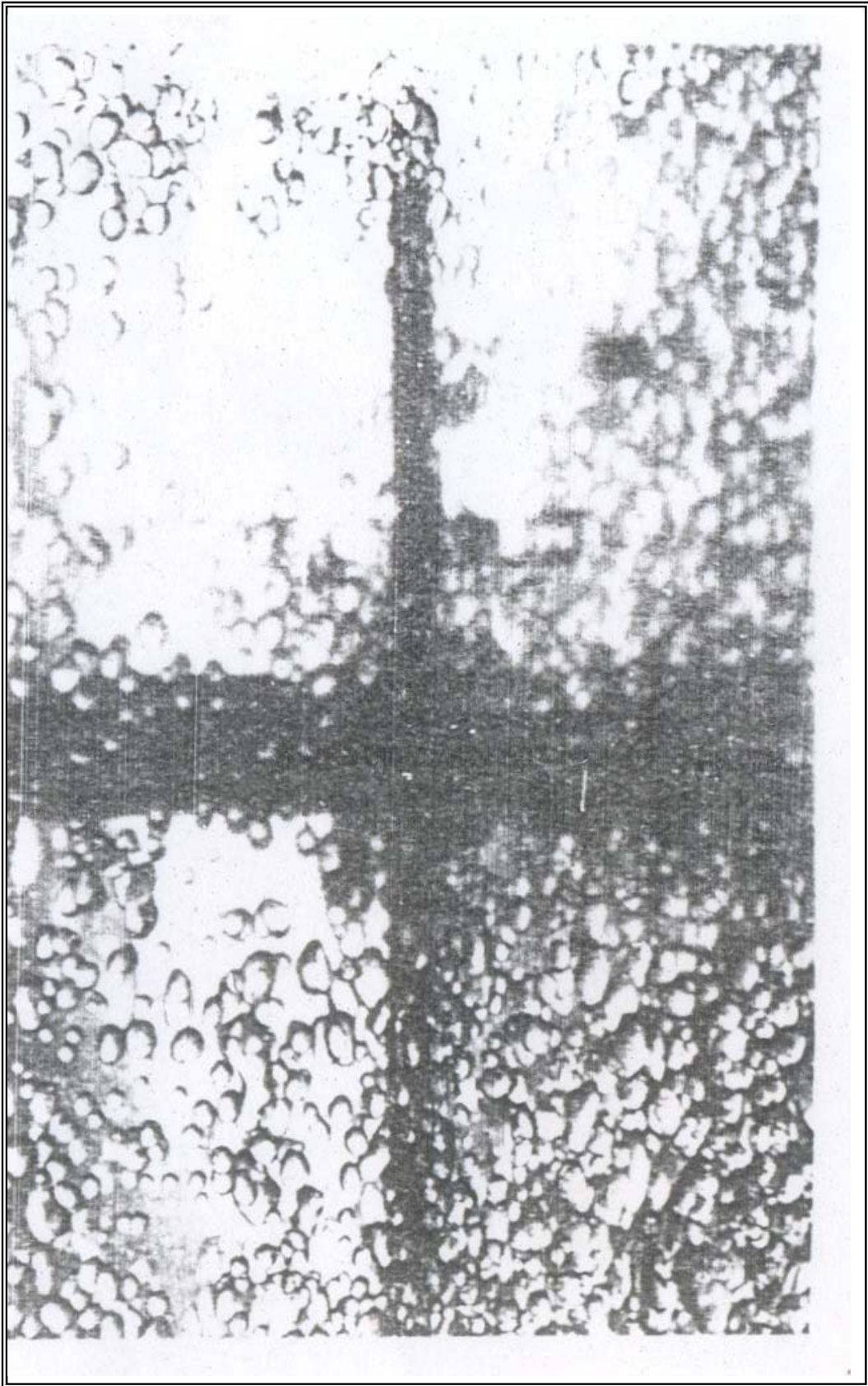


Fig. 3.2 Continuous and Dispersed Phases

3.6.2 Theoretical mass Transfer Coefficient

The method of calculation of dispersed phase transfer coefficient K_{cal} was used, these calculations involve the use of the drop distribution diagram to determine the volume percentage of stagnant, circulating and oscillating drops, in drop swarms. Sample population, and Droplet Reynolds number have been used as a measure of the state of drops, as follows :

Stagnant drops $Re < 10$

Circulating drops $10 < Re < 200$

Oscillating drops $Re > 200$

Where droplet Reynolds number is:

$$Re = \frac{d\rho V_c}{\mu_c} \quad (3.7)$$

where d is the drop diameter and V_c is vertical relative velocity of drops determined by applying Misesk equation:

$$V_c = \left[\frac{V_d}{x} + \frac{V_C}{1-x} \right] \quad (3.8)$$

To find the maximum diameter of stagnant drops in the whole drop population:

set $Re = 10$

$$\frac{d_s \rho c V_c}{\mu c} = 10 \quad (3.9)$$

where d_s is maximum diameter of the stagnant drops regime, to find the minimum diameter of oscillating drops in the oscillating drop regime:

set $Re = 200$

$$\frac{d_o \rho c V_c}{\mu_0} = 200 \quad (3.10)$$

where d_o is the minimum diameter of the oscillating drops regime. The circulating drops regime is determined some what between d_s and d_o , the stagnant drops are too small to be analyzed by the technique used in this study, so the drop population was considered to contain circulating

and oscillating drops only within the boundary between regimes, the sauter mean diameter is calculated from the following equation :

$$d_{32} = \frac{\sum nidi^3}{\sum nidi^2} \quad (3.11)$$

(i) Circulating drops regime

Volume percentage of the circulating drops was determined from the drop distribution diagrams and individual mass transfer coefficient of the dispersed and continuous phase for the circulating drop were calculated as

- (a) Dispersed phase mass transfer coefficient was estimated by the Krong and Brink equation (Kronig et al 1960):

$$K_{dc} = \frac{17.9D_d}{dc} \quad (3.12)$$

Where dc is circulating drop mid-sector and D_d is the molecular diffusion of hexane in dispersed phase

- (b) Continuous phase mass transfer coefficient was estimated by Garner et al correlation equation (Garner et al 1959):

$$\frac{K_{c.c}\bar{d}_c}{D_c} = -126 + 1.8 \text{Re}^{0.5} Sc^{0.42} \quad (3.13)$$

where D_c is the molecular diffusion of hexane in continuous phase. The overall mass transfer coefficient of the circulating drops K_{os} is calculated as:

$$\frac{1}{K_{oc}} = \frac{1}{K_{dc}} + \frac{m}{K_{cc}} \quad (3.14)$$

The result of the calculation drop coefficient is shown in table (4.20)

(ii) Oscillating drops regime:

The set of the drop population was considered in the oscillating drop regime. The individual mass Transfer coefficient of the dispersed and continuous phase for this regime was calculated as follows:

- (a) Dispersed phase mass transfer coefficient was first estimated by Rose and Kintner (Rose et al 1966) .

$$K_{d.o} = 0.45(D_d\phi)^{0.5} \quad (3.15)$$

Where ϕ is the frequency of oscillating.

- (b) Continuous phase mass Transfer coefficient was estimated by Garner et al correlation equation (Garner et al 1960)

$$\frac{K_{c.o}\bar{d}_o}{D_c} = 50 + 0.0085 \text{Re}Sc^{0.7} \quad (3.16)$$

The over all mass transfer coefficient of oscillating drop $K_{o.o}$ was first estimated as follows:

$$\frac{1}{K_{o.o}} = \frac{1}{K_{d.o}} + \frac{m}{K_{c.o}} \quad (3.17)$$

Where $K_{d.o}$ is the dispersed phase coefficient calculated by Rose and Kintner equation secondly by Angel et al equation

$$K_{o.o} = K_{d.o} \left[\frac{1}{\sqrt[1+m]{\frac{D_d}{D_c}}} \right] \quad (3.18)$$

Where $K_{d.o}$ is the dispersed phase coefficient which is calculated by Angelo et al, the theoretical mass transfer coefficient for the whole drop population was calculated by:

$$K_{cal} = K_{o.c}V + K_{o.o}(1-V) \quad (3.19)$$

Two values of K_{cal} were obtained from the experiment,. This corresponds to two values of $K_{o.o}$ first from Rose et al and Garner et al correlation and secondly $K_{o.o}$ from Angelo et al correlation presenting K_{cal} value together with the experimental K .

CHAPTER FOUR

Results and Discussion

4.1 Result

Analysis of results were carried to determined the drop size, drop size distribution and the mass transfer coefficients using various models, namely by Rose and Angelo (1966) were determined. The concentration profiles were measured along the column through sample points. The results are shown in the tables (4.10) through (4.25). Experiments without mass transfer were first carried out to investigate and determine the operating hydrodynamics namely flooding at various phase ratios and speed of agitation. Eighty five percent of flooding velocity was selected and the column had been operated at this level for all experiments. Both the phase ratio and agitator speeds were varied in table (4.1)

Table (4.1).Determination of flooding points at different speeds.

Continuous phase rate g/min	At 200 Rpm	At 300 rpm	At 500 rpm	At 600 rpm
	Dispersed phase rate g/min			
100	770	640	502	420
200	650	510	447	310
300	500	440	325	210
400	420	318	280	140
500	317	210	160	102
600	225	160	106	90

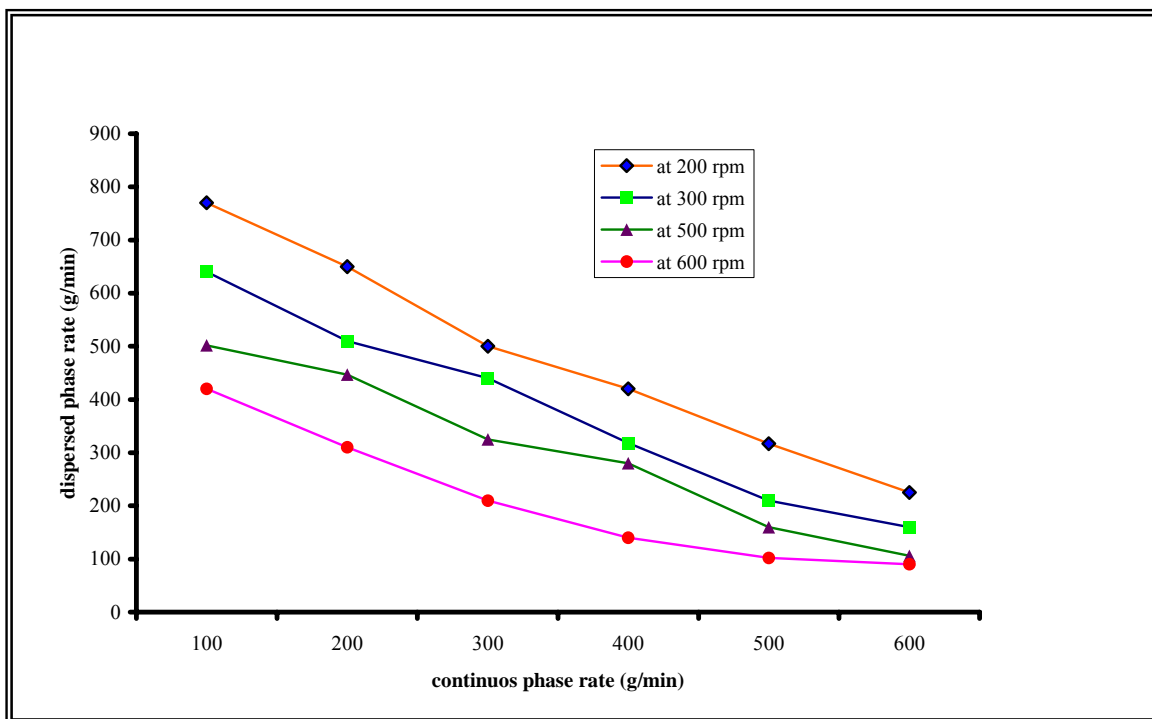


Fig.(4.1) Flooding points at different phase ratio and various agitator speeds(without mass transfer)

**Table (4.2) Drop size, number of drops and Cumulative volume at
200 rpm(without mass transfer)**

d_m mm	d mm	n	V mm³
1.400	1.0570	2	1.2367
2.5900	1.2950	4	4.5462
3.1400	1.5700	3	6.0757
3.700	1.8500	6	19.8813
5.3500	2.6750	7	70.1210
7.0100	3.5050	10	225.3422
6.1800	3.0900	9	466.4100
7.5600	3.7800	8	692.6472
7.8400	3.9200	10	1008.0437
8.1100	4.0550	7	1252.4257
8.1900	4.0950	8	1540.0664

Where:

d_m: Measured Diameter

d: Actual Diameter

n: Number of Drops

V: Cumulative Volume

Cumulative drop volume $V = \frac{\pi}{6} n \times d^3$

Phase ratio = 1: 0.8

Magnification= 2

**Table (4.3) Determination of Sauter mean diameter (d_{32})Agitator
Speed 200 rpm(without mass transfer)**

d_{mm}	d^2 mm^2	d^3 mm^3	n	nd^2 mm^2	nd^3 mm^3
1.0570	1.1172	1.1809	2	2.2344	2.3618
1.2950	1.6770	1.1717	4	6.7080	4.6868
1.5700	2.4645	3.8699	3	7.3935	11.9097
1.8500	3.4225	6.3316	6	20.5350	37.9896
2.6750	7.1556	19.1413	7	50.0892	133.9891
3.5050	12.2850	43.0590	10	122.8500	430.5900
3.0900	9.5481	29.5036	9	85.9325	265.5324
3.7800	14.2884	54.0102	8	114.3072	432.0816
3.9200	15.3664	60.2363	10	153.6640	602.3630
4.0550	16.4430	66.6765	7	115.1010	466.7355
4.0150	16.1202	64.7272	8	128.9618	517.7816
				807.7766	2906.021

$$d_{32} = 3.5975$$

**Table (4.4) Drop size, number of drops and Cumulative volume at
300 rpm (without mass transfer)**

d_m mm	d mm	n	V mm^3
2.0400	1.0200	4	2.2226
3.1400	1.5700	5	12.3540
3.700	1.8500	5	28.9302
4.8000	2.4000	3	50.6449
5.3200	2.6750	9	140.8461
3.9000	2.9500	10	275.2663
6.1800	3.0900	6	367.9547
6.4600	3.2300	8	509.1097
7.0100	3.505	5	621.8379
7.5600	3.780	5	763.2361
8.1100	4.0550	6	972.7064
8.1900	4.0950	5	1152.4818

**Table (4.5) Determination of Sauter mean diameter (d_{32}) Agitator
Speed 300 rpm (without mass transfer)**

d_{mm}	d^2 mm^2	d^3 mm^3	n	nd^2 mm^2	nd^3 mm^3
1.0200	1.0404	1.0612	4	4.1616	4.2448
1.5700	2.4649	3.8699	5	12.32415	19.3495
1.8500	3.4225	6.3316	5	17.1125	31.6580
2.4000	5.7600	13.8240	3	17.28	41.4720
2.6750	7.1556	19.1413	9	64.4004	172.2717
2.9500	8.7025	25.6724	10	87.025	256.724
2.0900	4.3681	9.1293	6	26.2086	54.7758
3.23	10.4329	33.6982	8	83.4632	269.5856
3.5050	12.8503	43.0590	5	64.2515	215.295
3.7800	14.2884	54.0102	5	71.442	270.051
4.0550	16.4430	66.6765	6	98.658	400.059
4.0950	16.7690	68.6692	5	83.8450	343.346
				614.172	2078.8324

$$d_{32} = 3.384773 \text{ mm}$$

**Table (4.6) Drop size, number of drops and Cumulative volume at
500 rpm (without mass transfer)**

d_m mm	d mm	n	V mm³
2.0400	1.0200	13	7.2234
3.1400	1.5700	9	25.4598
3.7000	1.8500	10	58.6121
4.2900	2.1450	8	99.9521
4.8000	2.400	7	150.6196
5.3500	2.6750	4	190.7090
6.1800	3.0900	8	314.2935
7.0100	3.5050	4	404.4761
7.5604	3.7805	3	431.4919
8.1100	4.055	2	501.3153
8.3900	4.1950	2	578.6233
8.66	4.3300	3	706.14484

**Table (4.7) Determination of Sauter mean diameter (d_{32}) Agitator
Speed 500 rpm (without mass transfer)**

d_{mm}	d^2 mm^2	d^3 mm^3	n	nd^2 mm^2	nd^3 mm^3
1.0200	1.0404	1.0612	13	13.5252	13.7856
1.5700	2.4649	3.8699	9	22.1841	34.8291
1.8500	3.4225	6.3316	10	34.22250	63.316
2.1450	4.6010	9.8692	8	36.8080	78.9536
2.4000	5.7600	13.824	7	40.3200	96.768
2.6750	7.1556	19.1413	4	28.6224	76.5652
3.0900	9.5481	29.5036	8	76.3898	236.0288
3.5050	12.2850	43.0590	4	49.1400	172.2360
3.7805	14.2922	54.0316	3	42.8766	162.0948
4.055	16.4430	66.6747	3	44.329	200.0241
4.1450	17.5980	73.5601	2	35.1960	147.1202
4.3300	18.7489	81.1827	3	56.2467	243.5481
				479.8578	1525.3837

$$d_{32} = 3.1788 \text{ mm}$$

Table (4.8) Drop size, number of drops and Cumulative volume at 600 rpm(without mass transfer)

d_m mm	d mm	n	V mm³
1.4900	0.7450	20	4.3301
2.0400	1.0200	15	12.6648
2.5900	1.2950	20	35.4073
3.1400	1.7500	8	51.6175
3.7000	1.8500	12	91.4003
2.2500	2.1250	3	106.4732
4.8000	2.400	2	120.9497
5.3500	2.6750	3	151.0167
5.9000	2.950	2	177.9007
6.1800	3.0900	3	224.2448

**Table (4.9) Determination of Sauter mean diameter (d_{32}) Agitator
Speed 600 rpm (without mass transfer)**

d_{mm}	d^2 mm^2	d^3 mm^3	n	nd^2 mm^2	nd^3 mm^3
0.7450	0.5550	0.4135	20	11.1000	8.2700
1.0200	1.0404	1.0612	15	15.606	15.9180
1.2950	1.6770	2.1717	20	33.54	43.434
1.5700	2.4649	3.8699	8	19.7192	30.9592
1.8500	3.4225	6.3316	12	41.0700	75.9792
2.1250	4.5156	9.5957	3	13.5468	28.7871
2.4000	5.7600	13.856	12	11.5200	27.648
2.6750	7.1556	19.1413	3	21.4668	57.4239
2.950	8.7025	25.6724	2	17.405	51.3448
3.0900	9.4581	29.5036	3	28.6443	88.5108
				213.6181	428.2678

$$d_{32} = 2.0048 \text{ mm}$$

Table (4.10) Drop size, number of drops and Cumulative volume at 200 rpm(with mass transfer)

d_m mm	d mm	n	V mm^3
1.49	0.745	3	0.6495
2.0400	1.0200	3	2.3164
2.5900	1.2950	4	6.849
3.4200	1.7100	5	19.9554
3.7000	1.850	5	36.5316
6.18	3.0900	6	129.2200
7.1000	3.5500	11	386.8974
7.2800	3.6400	8	5880.9167
7.5600	3.7800	10	871.7132
7.8400	3.9200	7	1092.4907
8.1100	4.055	8	1371.7844
8.3900	4.1950	7	1642.36244
8.66	4.3300	12	2152.4486
8.94	4.4700	16	2390.6209

**Table (4.11) Determination of Sauter mean diameter (d_{32}) Agitator
Speed 200 rpm(with mass transfer)**

d_{mm}	d^2 mm^2	d^3 mm^3	n	nd^2 mm^2	nd^3 mm^3
0.745	0.5550	0.4135	3	1.6650	1.2405
1.0200	1.0404	1.0612	3	3.1212	3.1836
1.2950	1.6770	2.1717	4	6.708	8.6868
1.7100	2.9241	5.0002	5	14.6205	25.0010
1.850	3.4225	6.3316	5	17.1125	31.658
3.0900	9.5481	29.5036	6	57.2886	177.0216
3.5500	12.6025	44.7389	11	138.6275	492.1279
3.6400	13.2496	48.2285	8	105.9968	38.828
3.78	14.2884	54.0102	10	142.8840	540.102
3.92	15.3664	60.2363	7	107.5648	421.6541
4.055	16.4430	66.6765	8	131.5940	533.412
4.1950	17.5980	73.8237	7	123.1860	516.7659
4.33	18.7489	81.1827	12	224.9868	974.1424
4.47	19.9809	89.3146	16	319.6944	1429.0336
				1451.208	5539.4074

$$d_{32} = 3.817101 \text{ mm}$$

Table (4.12) Drop size, number of drops and Cumulative volume at 300 rpm (with mass transfer)

d_m mm	d mm	n	V mm ³
2.5900	1.2950	1	1.1240
3.1400	1.5700	7	15.3079
3.700	1.8500	8	41.8297
4.2500	2.1250	10	92.0727
4.8000	2.4000	8	149.9785
5.1900	2.5950	7	214.0270
3.3500	1.6750	24	273.0817
6.4600	3.2300	15	537.7473
7.0100	3.505	9	740.6581
7.5600	3.7800	3	825.4970
8.1100	4.0550	2	895.3204
8.6600	4.3300	3	1022.8414

Table (4.13) Determination of Sauter mean diameter (d_{32}) Agitator Speed 300 rpm (with mass transfer)

d_{mm}	d^2 mm^2	d^3 mm^3	n	nd^2 mm^2	nd^3 mm^3
1.2950	1.6770	2.1717	2	1.6770	2.1717
1.5700	2.4649	3.8699	7	17.2543	27.0893
1.8500	3.4225	6.3316	8	27.3800	50.6528
2.1250	4.5156	9.5957	10	45.1560	95.9570
2.4000	5.7600	13.824	8	46.08	110.592
2.5950	6.7340	17.4748	7	47.1380	122.3236
1.6750	2.8056	4.6994	24	67.3344	112.7856
3.2300	10.4329	33.6982	15	156.4935	505.473
3.505	12.2850	43.590	9	110.5650	387.531
3.7800	14.2889	54.0402	3	42.8652	162.0306
4.0550	16.4430	66.6747	2	32.8860	133.3494
4.33	18.7489	81.1827	3	56.2467	243.5481
				651.2964	1953.5046

$$d_{32} = 2.9994 \text{ mm}$$

Table (4.14) Drop size, number of drops and Cumulative volume at 500 rpm (with mass transfer)

d_m mm	d mm	n	V mm^3
2.59	1.2950	14	15.91973
3.1400	1.5700	10	36.1824
3.1700	1.5850	17	71.6280
3.70000	1.8500	10	104.7803
4.2300	2.1150	12	164.2247
5.350	2.6750	3	194.2917
5.9000	2.9500	5	261.5018
6.4600	3.2300	4	305.0781
7.0100	3.5050	3	327.6237

Table (4.15) Determination of Sauter mean diameter (d_{32}) Agitator Speed 500 rpm (with mass transfer)

d_{mm}	d^2 mm^2	d^3 mm^3	n	nd^2 mm^2	nd^3 mm^3
1.2950	1.6770	2.1717	14	23.478	30.4038
1.5700	2.4649	3.8899	10	24.349	38.6990
1.5850	2.5122	3.9819	17	42.7074	67.6923
1.8500	3.4225	6.3316	10	34.2250	63.31600
2.1150	4.4732	9.4609	12	53.6784	113.5308
2.6750	7.1556	19.1413	3	21.4668	57.4239
2.950	8.7025	25.6724	5	43.5125	128.362
3.23	10.4329	33.6982	4	41.7316	134.7928
3.5050	12.2850	43.0590	3	37.755	129.177
				323.2037	763.3976

$$d_{32} = 2.3619 \text{ mm}$$

Table (4.16) Drop size, number of drops and Cumulative volume at 600 rpm (with mass transfer)

d_m mm	d mm	n	V mm^3
1.4900	0.7950	25	6.5772
2.0400	1.0200	18	16.5788
2.4200	1.2100	10	25.8547
2.5900	1.2950	21	49.7343
3.1400	1.5700	11	72.0233
3.1700	1.5850	9	90.7875
3.7000	1.8500	7	113.9941
4.2500	2.1250	4	134.0913
5.9000	2.9800	3	175.6602

**Table (4.17) Determination of Sauter mean diameter (d_{32}) Agitator
Speed 600 rpm (with mass transfer)**

d_{mm}	d^2 mm^2	d^3 mm^3	n	nd^2 mm^2	nd^3 mm^3
0.7950	0.6320	0.5025	25	15.8000	12.5625
1.0200	1.0404	1.0612	8	18.7272	19.1016
1.2100	1.4641	1.7716	10	14.641	17.716
1.2950	1.6770	2.1717	21	35.217	451.057
1.7500	2.4649	3.8699	11	27.1139	42.5689
1.5850	2.5122	3.9819	9	22.6098	35.8371
1.8500	3.4225	6.3316	7	23.9575	44.3212
2.1250	4.5156	9.5957	4	18.0624	38.3828
2.9800	8.8804	26.4836	3	26.6412	79.4508
				202.765	335.5538

$$d_{32} = 1.6548 \text{ mm}$$

Table . (4.18)Experimental Mass Transfer Results

Run No.	N gm/s	d ₃₂ cm	Interfacial Area cm ²	C _m gm/cm ³	K _{EXP} cm/s
1	3.67	0.38171	73334.7	0.0206	3.59 × 10 ⁻³
2	1.87	0.29994	9469.07	0.008	3.01 × 10 ⁻³
3	1.62	0.23619	63245.88	0.0129	3.10 × 10 ⁻³
4	1.35	0.16548	230601.6	0.0119	3.34 × 10 ⁻³
5	1.60	0.3575	49765.86	0.0109	3.32 × 10 ⁻³
6	3.80	0.33847	82660.5	0.0109	3.42 × 10 ⁻³
7	5.38	0.31788	71978.22	0.0139	2.92 × 10 ⁻³

Where :

N = Rate of mass transfer.

ΔC_m = The mean driving force.

K_{EXP} = Mass transfer coefficient.

Specific interfacial area $a = \frac{6x}{d_{32}}$

Total interfacial area A = a . v

$$K_{EXP} = \frac{N}{A \times \Delta C_m}$$

**Table . (4.19)Theoretical Mass Transfer Results ,Result of Calculation
of V_0 and d_s and d_0**

Run No.	Dispersed phase	V_0 cm/sec	d_s cm	d_0 cm
1	n-hexane	9.143	0.015	0.303
2	“	8.51	0.012	0.240
3	“	9.62	0.0106	0.212
4	“	9.44	0.0103	0.205
5	“	10.14	0.00100	0.200
6	“	10.36	0.0098	0.197
7	“	10.45	0.0097	0.195

Where:

d_s = Diameter of stagnant drop.

d_0 = Diameter of oscillating drop.

The vertical relative velocity of drops $V_0 = \left[\frac{v_d}{X} + \frac{v_c}{1-X} \right]$

Table . (4.20) Mass Transfer Results
Circulating drop mass transfer coefficient

Run No.	Dispersed phase	K_{dc} Cm/sec	K_{cc} cm/sec	K_{oc} cm/sec
1	n-hexane	9.6×10^{-6}	1.26×10^{-3}	9.53×10^{-6}
2	“	1.26×10^{-5}	1.56×10^{-3}	1.25×10^{-5}
3	“	1.37×10^{-5}	1.73×10^{-3}	1.36×10^{-5}
4	“	1.47×10^{-5}	1.85×10^{-3}	1.46×10^{-5}
5	“	1.8×10^{-5}	2.54×10^{-3}	1.79×10^{-3}
6	“	2.27×10^{-5}	2.24×10^{-3}	2.25×10^{-5}
7	“	2.23×10^{-5}	2.28×10^{-3}	2.21×10^{-5}

Where:

K_{dc} = Dispersed phase mass transfer coefficient of circulating drop.

K_{cc} = Continuous phase mass transfer coefficient of circulating drop.

K_{oc} = Overall mass transfer coefficient of circulating drop.

Table . (4.21) Mass Transfer Results
Comparison between mass transfer coefficient
With different models

Run No.	Dispersed phase	Rose et al		Angelo et al	
		K_{d0}	$K_{0.0}$	$K_{0.0}$	$K_{d.0}$
1	n-hexane	2.78×10^{-3}	4.03×10^{-5}	3.31×10^{-3}	2.8×10^{-3}
2	-	3.93×10^{-3}	3.93×10^{-6}	3.53×10^{-3}	7.14×10^{-3}
3	-	2.87×10^{-3}	2.87×10^{-3}	3.82×10^{-3}	7.72×10^{-3}
4	-	2.94×10^{-3}	2.94×10^{-3}	3.90×10^{-3}	7.88×10^{-3}
5	-	1.92×10^{-3}	1.91×10^{-3}	2.62×10^{-3}	5.30×10^{-3}
6	-	3.02×10^{-3}	3.21×10^{-3}	3.99×10^{-3}	8.07×10^{-3}
7	-	2.67×10^{-3}	2.23×10^{-3}	4.02×10^{-3}	8.14×10^{-3}

Where:

K_{d0} = Dispersed phase mass transfer coefficient of oscillating drop.

$K_{0.0}$ = Overall mass transfer coefficient of oscillating drop.

Table . (4.22) Mass Transfer Results, Comparison between mass transfer coefficient with various conditions

K_{exp} Cm/sec	K_{dc} cm/sec	K_{cc} cm/sec	K_{oc} cm/sec	K_{do} Rose et al	K_{do} Angelo et al
3.59×10^{-3}	9.6×10^{-6}	1.26×10^{-3}	9.53×10^{-6}	2.78×10^{-3}	2.8×10^{-3}
3.01×10^{-3}	1.2×10^{-5}	1.56×10^{-3}	1.25×10^{-5}	3.93×10^{-3}	7.14×10^{-3}
3.10×10^{-3}	1.37×10^{-5}	1.73×10^{-3}	1.36×10^{-5}	2.87×10^{-3}	7.72×10^{-3}
3.34×10^{-3}	1.47×10^{-5}	1.80×10^{-3}	1.46×10^{-3}	2.94×10^{-3}	7.88×10^{-3}
3.32×10^{-3}	2.27×10^{-5}	2.04×10^{-3}	1.79×10^{-3}	1.42×10^{-3}	5.30×10^{-3}
3.42×10^{-3}	1.8×10^{-5}	2.29×10^{-3}	2.25×10^{-3}	3.02×10^{-3}	8.07×10^{-3}
2.92×10^{-3}	2.23×10^{-5}	2.28×10^{-3}	2.21×10^{-3}	2.67×10^{-3}	8.14×10^{-3}

Table No. (4.23) Experimental and theoretical over mass transfer coefficient

Run No.	K_{exp} cm/sec	K_{cal} Rose and Garner	K_{cal} Angelo et al
1	3.59×10^{-3}	3.11×10^{-5}	2.32×10^{-3}
2	3.01×10^{-3}	8.74×10^{-6}	2.97×10^{-3}
3	3.10×10^{-3}	1.48×10^{-3}	2.68×10^{-3}
4	3.34×10^{-3}	1.49×10^{-3}	3.17×10^{-3}
5	3.32×10^{-3}	1.87×10^{-3}	2.27×10^{-3}
6	3.42×10^{-3}	1.55×10^{-3}	2.79×10^{-3}
7	2.92×10^{-3}	1.57×10^{-3}	2.82×10^{-3}

Where:

K_{cal} = Calculated mass transfer coefficient.

Table. (4.24) Comparison between experimental and theoretical mass Transfer coefficients

Dispersed phase	$\frac{K_{exp}}{K_{Cal}}$ Rose	$\frac{K_{exp}}{K_{Cal}}$ Angelo	$\frac{K_{exp}}{K_{0.0}}$ Angelo	$\frac{K_{exp}}{K_{0.0}}$ Rose
n-hexane	115.43	1.54	1.08	89.08
“	344.39	1.01	0.85	421.56
“	2.09	1.15	0.81	1.49
“	2.24	1.05	0.85	1.57
“	1.77	1.46	1.26	1.73
“	2.20	1.22	0.85	1.54
“	1.85	1.03	0.72	0.76

Table .(4.25) Mass Transfer Results
Comparison between experimental and theoretical mass
Transfer coefficients

Run No.	K_{exp} Cm/sec	K_{cal} by Rose cm/sec	K_{cal} by Angelo cm/sec	$\frac{K_{exp}-k_{cal} \times 100}{K_{exp}}$ Rose	$\frac{K_{exp}-k_{cal} \times 100}{K_{exp}}$ Angelo
1	3.59×10^{-3}	3.11×10^{-5}	2.32×10^{-3}	99.13 %	35.37 %
2	3.01×10^{-3}	8.73×10^{-6}	2.97×10^{-3}	99.75	1.32
3	3.10×10^{-3}	1.45×10^{-3}	2.68×10^{-3}	53.22	13.54
4	3.34×10^{-3}	1.44×10^{-3}	3.17×10^{-3}	55.38	5.08
5	3.32×10^{-3}	1.87×10^{-3}	3.27×10^{-3}	43.67	1.50
6	3.42×10^{-3}	1.55×10^{-3}	2.29×10^{-3}	54.67	18.42
7	2.92×10^{-3}	1.57×10^{-3}	2.82×10^{-3}	46.23	3.42

4.2 Discussions

In general the waste water from oil fields and refineries has considerable amount of crude oil fields in an emulsified and tiny floating

forms. These oil/water emulsions must be separated to recover the oil , used the oil free water for agriculture and protect the environment from oil pollution. Therefore One of objectives, of this work is to investigate the extraction of oil from an oil/water emulsion by an organic solvent in a pilot sieve tray column. The oil emulsion was first made as continuous phase were the column was filled with the mixture, agitation

started and the organic solvent was then introduced at the bottom of the column as a dispersed phase. Due to agitation small drops of oil/water were formed, these drops get into contact with the organic solvent and because of high solubility of the oil in the organic phase, the oil within the drop was mixed with the solvent and removed from the drop leaving the water to bind with the water in the continuous water phase and thus being separated, and the drops disappeared. This separation is found to be a function of drop size and drop size distribution, which were mainly function of the speed of agitation that was varied from 200 to 600 rpm above which the system became hazy. , The drop size was measured and the oil concentration profiles were determined. It was observed that the direction of mass transfer was always from the oil/water emulsion to the organic phase. This is because the oil content within the drop was not like a normal solute in solvent extraction in which the solute transfer depends on the difference in solubility and selectivity in both phases. Here the situation is different and the oil in the emulsion is partially soluble with the water and bound to it by physical forces and by partial solubility of the emulsified part of the oil.

4.2.1 Column Hydrodynamics

Experiments were carried out to investigate the various factors on column hydrodynamics without oil transfer. Drop size and drop size

distribution were studied at different agitator speed (200 – 600 rpm) at specified feed rates and phase ratios. The results indicated that drop size decreased with agitator speed which is in agreement with all previous works. Initially large drop size were dominant at low speeds, but still drop size appeared, such drops might be due to the fact that these were the smallest drop, which did not undergo any change as their size were already established and could not be further subdivided into smaller drops. However, upon increasing the agitator speed, the smaller size droplets become dominant and increased in population, this decrease in drop size continued to decrease with speed of agitation, until a maximum speed was reached (600 rpm) when the drop size could no longer be reduced. Any further increase in the agitator speed will make the system milky and hazy and at further speeds flooding occur, flooding was defined by phase ratio $n_{\text{hexane}}/emulsion$ in all cases i.e. at all feed rates, phase ratios with either phase dispersed, the agitator speed played a controlling point with regard to the flooding determination and as the phase ratio increased, flooding occurred at a comparatively lower speed, the same effect was realized with the feed rate i.e. as the feed rate increased.

A difference was clearly seen, when comparing the agitator speed at which flooding occurred with respect to each dispersion, and when emulsion was dispersed, flooding occurred at higher speed than that producing flooding when n.hexane was dispersed at same conditions. This is because the agitator speed needs more energy to disperse the heavy phase than that required to disperse the light phase, hence flooding occurred at higher speed.

The centrifugal action of the agitator tended to make the light phase flow to the centre of the column and when the heavy phase was dispersed it was necessary to overcome, the centrifugal action by setting up a high velocity flow pattern to bring the heavy phase into the area in which the

agitator was effective. Hence, the speed required to disperse the heavy phase into light phase was much higher than that required to disperse the light phase into the heavy phase.

Experiments showed that as the phase ratio was increased, flooding occurred at lower speed. The opposite was also true i.e as the phase ratio decreased, flooding occurred at higher speed, at flooding, both the phase ratio or the agitator speed may be used to get the column back to normal operation conditions. This could be made by lowering the agitator speed. However, if lowering the agitator speed does not eliminate flooding appearance, the phase ratio must be lowered or both the phase ratio and agitator speed, should be lowered to eliminate flooding.

4.2.2 Analysis of Results:

A series of experiments were carried out to investigate the effect of the various parameters on sieve tray column performance.

These factors were

- A. Solvent emulsion ratio
- B. Speed of agitator
- C. Feed flow rate

The results indicated that the effects of the oil/emulsion ratio was significant, thus increasing the ratio will increase separation efficiency.

The concentration of the oil in the emulsion feed is an important factor in the determination of the column hydrodynamics. it was also found that the speed of agitation was significant table(4.2). As the speed was increased to a higher level its effect on the droplets size is dominant but particular consideration should be given to the column hydrodynamic as the column approaches flooding.

It appears that by increasing the agitator speed, the droplet size decreases and the relevant dispersion is improved (smaller drop diameter) and consequently the transfer area increases. However a further increase in

the agitator speed did not increase the interfacial area as a uniform drop size had been already established.

4.2.3 Experimental mass transfer coefficient

The overall experimental dispersed phase mass transfer coefficients recorded in this study were evaluated by Simpson's rule. Simpson's rule has a great advantage over the log-mean driving force in the agitated column. The agitator speed causes more the drop to break-up and the proportion of the small droplets will be greater while the mass transfer coefficient become smaller, with the result that stagnant or circulating droplets replace some oscillating drops. The real gain in the higher energy is in the interfacial area which increases more rapidly than the decrease in mass transfer coefficients.

4.2.4 Theoretical mass transfer coefficient

Since fairly wide range of drop size exists in the dispersion in agitated extractor, it is likely that more than one transfer mechanism would take place over the wide spectrum of drop sizes. Therefore the assumption of uniform drop size could lead to serious errors when interpreting mass transfer and related processes.

The mass transfer coefficient calculation by Rose and Kintner and Garner equations as shown in table (4.22) The value of K_{cal} were compared in table (4.24) as K_{exp}/K_{cal} , it is found that the ratio vary from 1.54 to 115.43 for the runs in which n-hexane dispersed and from 1.08 to 89.08 when the emulsion was dispersed. This wide range of difference may be due to the large proportion of circulating drops.

The experimental mass transfer coefficients were generally lower for lower phase flow rates than those at higher flow rates at identical agitator speed. The flow rate effect is shown by the following equations:

$$Sh_c = -126 + 1.8(Re)^{0.5} (Sc)^{0.42} \quad (4.1)$$

$$Sh_c = 50 + 0.0065(Re)(Sc)^{0.7} \quad (4.2)$$

where Reynolds number $\left(\frac{d\rho_c V_0}{\mu}\right) V_0$ is calculated by Misck's equation:

$$V_0 = \left[\frac{V_d}{X} + \frac{V_c}{1-X} \right] \quad (4.3)$$

which relates the phases velocities with hold up volume.

The mass transfer coefficient calculated by Anglo et al are compared in table (4.24) as a ratio of $K_{\text{exp}}/K_{\text{cal}}$

The comparison ratio deteriorate at lower phases flow rates and this might be attributed to the inadequate allowance for phase flow rate in the equation. This is due to the fact that the contribution of the oscillating drops regime is very small.

Theoretically overall mass transfer coefficients were generally reasonable compared with experimental coefficients and the ranges of the ratios between the coefficient ($K_{\text{exp}}/K_{\text{cal}}$) is very narrow compared with that previously reported by AL Hamiri, where no stagnant drops were included in calculation. However, they exist in dispersion but their contribution to the overall mass transfer coefficient will be insignificant because the proportion will be very small within the whole drop population.

The use of Reynolds number, as measure of state of the drops in classifying them as stagnant, circulating and oscillating drops is adequate for accurate classification in agitated systems.

Finally table (4.25) shows the comparison of $\frac{K_{\text{exp}} - K_{\text{cal}}}{K_{\text{exp}}}$, the result shows that the model made by Anglo et al gave better result than Rose and Garner model.

Hence the model of Anglo et al is recommended to be used for the prediction of mass transfer coefficient in this type of columns

CHAPTER FIVE

CONCLUSION AND RECOMMENDATIONS

- It is concluded that

Both drop size and dispersed phase holdup are different when mass transfer occurring is compared to non mass transfer. Therefore data obtained under nonmass transfer conditions must be applied with caution in column design .

- Direction of mass transfer

With the system studies oil transfer from dispersed to continuous phase enhanced coalescence with larger drop size and less holdup and vice versa.

- Experimental overall mass transfer coefficient

The use of the driving force profile along the column to calculate the mean driving force through Simpson's rule results in a more precise experimental overall mass transfer coefficient.

- Theoretical over all mass transfer coefficient with drop size distribution

The use of drop size distribution in the calculation of theoretical overall mass transfer coefficient gives results that are in agreement with the experimental coefficients and methods of calculations stated in section 3.7 represent a first step in making such calculations more rigorous without drop distribution.

The wide diversion in the calculated mass transfer coefficient from that of the experimental coefficient K_{EXP} confirms that different mass transfer mechanisms occur simultaneously and that drop size distribution must be included in calculation process.

-Mass transfer coefficient models

The oscillating drop mass transfer coefficient models of Rose et al and Garner et al generally give closer results to the experimental coefficient.

5.2 recommendation

- The prediction of drop size and dispersed phase under mass transfer condition are less reliable using the correlation developed for nonmass transfer conditions.
- To improve the calculation of theoretical overall mass coefficients with involvement of drop size distribution, more work is needed to find a new

basis for classifying the state of drop viz stagnant, circulating, or oscillating in agitated contactor.

- The effect of the axial, mixing in either phase or both, on the column performance has long been one of major problem encountered in agitated extractor operation. Therefore quantitative assessment of this phenomenon would be very useful.
- The factors that affect mass transfer rate and mass transfer coefficients were investigated in a sieve tray column, these are the drop size , drop size distribution, and agitator speed. It was found that the rate of mass transfer is affected by all these factors. Different models have been used to predict mass transfer coefficients and model formulated by Angelo et al was applied and compared with that modeled by Rose and Garner. It is confirmed that the model formulated by Angelo et al gave less diversion form the experimental mass transfer coefficient in comparison with that of Rose and Garner. The result predicted by the above mentioned models confirmed the superiority of Angelo et al based on this result, Angelo et al model is recommended to be used for prediction of mass transfer coefficient in liquid-liquid extraction equipment such as sieve tray column and other similar equipments.

REFERENCES

1. Sherwood, T. K. et al, Ind, Eng. Chem (1939)
2. Jeffreys, G. V. and Ellis, E. M. R (1962).
3. Sawistowski H. and Gotz, G. E. Trans. Ind Chem. Eng (1963).
4. Skelland A. H. P. and Minhas, S. S. A. 1971.
5. Heertjes, P. A. and de Wie, L. H. Chem. Eng. (1966).
6. Coulson, J. H. and Skinner, S. J. Chem. Eng, 1951
7. Poporich, A. T. Jervis, R. E. and Trass, O. Chem. Eng. (1969).
8. Heertjes, P. M. and De Wie, L. H. Mass Transfer to Drop, Recent, Advances, in liquid-liquid Extraction. Edited by Hanson, C. Pergamon Press (1971).
9. Rose, P. M. and Kintner, R. C., A. I. Ch, E. Inc. (1966).
10. Angelo, J. b. Lightfoot E. W. and Howard, O. W. A. T. chem. Eng. Ind. (1966).
11. Forsyth, J. S. et al, Ind Solvent Conf (1974).
12. Garner, F. H. and Tayeban, H. Soc. 1962.
13. Hadamard, C. R. and Rybezynski, A. Acad Sci Paris (1911).
14. Levich. V. Shur. Obstch. Khim. (1949).
15. Garner F. H. and Skelland, A. M. P. Chem. Eng. Sc. (1955).
16. Al-Hassan, T. S. Ph. D. Thesis, University of Aston in Birmingham U. K (1979).
17. Newman, A. B. Trans. Am. Inst. Chem. Eng (1931).
18. Vermulen, T. Ind. Eng. Chem. (1953).
19. Treybal, R. E. Liquid Extraction, McGraw-Hill new York 2nd Edition (1963).
20. Kranig, R. and Brink, T. C. App. Sci. Res. (1960).
21. Calderbank P. H. and Korchinski, I. T. O. Chem. Eng. Sci (1956).
22. Handlas, A. E. and Baron, T. A. (1957).

23. Skelland, A. H. P. and Wellek, R. H (1964).
24. Johnson, A. I. And Hamleec. A. E. (1960).
25. Olander, D. R. A. I. Ch. E. Ind. (1966).
26. Gunn. R. Jni. Geophys. Res. (1949).
27. Garner, F. H. and Haycock, P. J.. (1959).
28. Johnson, AI and Hamleec, A. E.,. Chem. Eng.Jnl 1960
29. Schroeder, R. R. and Kintner, A. R. C. A. K. chem Ind. (1956).
30. Ellis, W. B., Ph. D. Thesis, University of Maryland U. S. A. (1966).
31. Linton, M. and Sutherland, Chem. Eng. Sci. (1960).
32. Sideman, S. and Shafrai, H. Chem. Eng. (1964).
33. Griffith, R. M. Chem. Eng. Sci. (1960).
34. Garner, F. H. and Suckling, R. D.,. (1968).
35. Rowe, P. N. et al, Trans. Ind. Chem. Engres (1965).
36. Kinard, G. E. Manning, F. S., and, Manning W. P. Chem. Eng. (1963).
37. Garner, F. H. Foord, A. and Tayeban, M. Appl. Chem., (1959).
38. Mekasut, Molinier. J. and Angelino, 14 Chem. Eng. Sci. (1978).
39. Yamaguchi, M. Watanabe. S and Katayama, T. Ind. Chem. Eng. Japan (1975).
40. Thorsen, G. et al Chem. Eng. Sci. (1968).
41. Groothuis, H. and Zwiderweg, F. J. Chem. Eng. Sci. (1960).
42. Sawistowski, H. Recent Advances in liquid-liquid extraction edited by Hanson, C. Pergamon Press W. T. (1971).
43. Al-Hemiri, A. A. A. Ph. D. Thesis University of Aston in Birmingham U. K. (1976).
44. Arnold, D. R. Ph. D. Thesis University of Aston in Birmingham U. K. (1974).
45. Mcferrin, A. R. and Davidson, R. R. (1971).
46. Johnson, A. I. And Haeies, A. E. Chem. Jns (1960).

47. Licht, W. and Conway, J. B. Int Eng. Chem. (1950).
48. Coulson, J. H. and Skinner, R. E. and Trass, O. Chem., Eng. (1969).
49. Mumford, C. J. Ph. D. Thesis University of Aston in Birmingham U. K. (1970).
50. Sternling, C. V. and Schriener, L. E. Chem. (1959).
51. Orell, A. and Westwater, J. W. A. J. Chem. Eng. Sc. (1962).
52. Maroudas, N. G. and Sawistowski, H. Chem. Eng. (1965).
53. Sarkar, S. Ph. D. Thesis University of Aston in Birmingham, U. K. (1976).
54. Sehr, B. and Linde, H. P. 3rd Berlin (1967).
55. Haydon, D. A. Proc. Soc. (1958).
56. Davies, J. T. "Turbulence Phenomena". Academic Press New York (1972).
57. Hoim, A. and Terjesen, S. G. Chem, Eng. (1955).
58. Sieicher, C. A. A. I. (19959).
59. Hartland, S. and Mechlenburgh, J. C. Chem. Eng. (1966).
60. Harkins, W. D. and Brown, F. E., Ind. (1919).
61. Treybal, R. E. and Howarth, C. B., Ind. Eng. Chem. (1950).
62. Kolmogoroff, A. N. Acad. (1991).
63. Hinze, J. O. I. A. (1955).
64. Ciay, P. H. Proc. Acad. (Amsterdam) (1990).
65. Strand, C. P. Oiney, R. B. and Akermam, G. H.
66. Lawson, G. B. Ph. D. Thesis University (1954), of Manchester 1967.
67. Howarth, W. J. Chem. Eng. (1966).
68. Khandelwal, A. N. Ph. D. Thesis, University of Aston in Birmingham, U. K. (1978).
69. Todd, D. B. Chem. Eng. (1969).

70. Logsdail, D. H. et al. "Recent advances in Liquid Extraction London (1971).
71. S.Sajjadi, M. Zerfa, B. W. Brooks, Dynamic behaviour of drops in oil/water oil dispersions. (2000)
72. Bently, B.J & Leal, L. G. An experimental investigation of drop deformation and breakup in steady, two- dimensional linear flows.(1986).
73. Cutter, L. A. flow and turbulence in a stirred tank. (1966).
74. Gopal, E. R. Emulsion science London Academic press. (1968).
75. Hong, P. O. & Lee, J. M. Unsteady- liquid-liquid dispersions in agitated vessels. (1983).
76. Al-saadi, A.N.and Jeffreys, G.V. chem..Eng. (1981)
77. Gurashi, A. G. Ph. D.Thesis , University of of Aston in Birmingham, U. K. (1985).
78. Othmer, D.F. and Tobias, P. E . ind .chem. Eng. (1942)
79. Hand, D. B. Phys.chem .(1930)
80. Rod, V. chem.. Eng. (1966)

Appendices

1. Calculation of over all mass transfer coefficients

1.1 The over all experimental mass transfer coefficient

X	Y	Y*	$\Delta Y : Y^* - y$
4.44	3.23	4.22	0.99
4.04	2.07	3.81	1.82
4.02	2.32	3.82	1.5
3.98	1.41	3.78	2.37
3.88	1.00	3.69	2.61
3.03	0.55	2.88	2.33
1.04	0.05	1.37	1.32

Equilibrium relationship $y^* = 0.95x$

X = Mass fraction of oil in emulsion.

Y = Mass fraction of oil in organic phase.

From table (4.17) $d_{32} = 0.38171$

Holdup volume $x = 5.5\% = 0.055$

Effective length of column = 120 cm

Density of emulsion = 0.977 g/cm^3

Agitation speed = 200 rpm

$$\text{Cross sectional area of the column } A = \frac{\pi D^2}{4} = \frac{3.14 \times 30^2}{4} = 706.5 \text{ cm}^2$$

The specific interfacial areas $a : \frac{6x}{d_{32}}$

$$a = \frac{6 \times 0.055}{0.3871} = 0.865$$

Total interfacial area.

$$A = a.v$$

$$A: 0.868 \times 120 \times 706.5 = 73334.7 \text{ cm}^2$$

Δy_{cm} The mean driving force was estimated by applying Simpson's rules as

$$\Delta y_m = \frac{1}{18} \{ \Delta y_{top} + \Delta y_{bot} + 4(\Delta y_2 + \Delta y_4 + \Delta y_6) + 2(\Delta y_3 + \Delta y_5) \}$$

$$\Delta Y_m = \frac{1}{18} [(0.99 + 1.32) + 4(1.82 + 2.37 + 2.33) + 2(1.5 + 2.61)] \\ = 2.063$$

$$\Delta C_m = \frac{2.063}{0.977 \times 100} = 0.0211$$

Rate of mass transfer

$$N = Q_d \rho_d (x_{in} - x_{out}) \\ = 0.977 \times 706.5 \times 0.0323 \times 0.25 = 5.57$$

$$K_{exp} = \frac{N}{A \cdot \Delta C_m} = \frac{5.57}{0.0211 \times 73334.7} = 3.59 \times 10^{-3} \text{ cm/sec}$$

Theoretical Overall mass Transfer Coefficient

The vertical relative velocity of drop V_o in the column determined by applying misek's equation

$$V_o = \left[\frac{V_d}{x} + \frac{V_c}{1-x} \right]$$

$$V_o = \frac{0.3}{0.035} + \frac{0.25}{1-0.035} = 7.02 \text{ cm/sec}$$

The maximum diameter of stagnant drops in the whole drop population where droplet Reynolds number $Re: 10$ was found from

$$\frac{d_s \rho_c V_o}{\mu_c} = 10$$

$$d_c = \frac{10 \times 0.0104}{0.977 \times 9.193} = 0.015 \text{ cm}$$

The minimum diameter of the Oscillating drop when $Re: 200$

$$d_o = \frac{200 \times 0.0104}{0.977 \times 7.2} = 0.303 \text{ cm}$$

circulating drops regime

A) Dispersed phase mass transfer coefficient was estimated by knowing and Brink equation

$$K_{dc} = \frac{17.9 D d}{d_c}$$

d_c = from drop size d_c :

from diffusion of hexane $D_d = 1.1298 \times 10^{-7} \text{ cm}^2/\text{sec}$.

$$K d_c = \frac{17.9 \times 1.298 \times 10^{-7}}{0.242} = 9.6 \times 10^{-6} \text{ cm/sec}$$

continuous phase mass transfer coefficient was estimated by Garner

$$\frac{K_{cc} d_c}{D_c} = 126 + 1.8 \text{ Re}^{0.5} \text{ Sc}^{0.42}$$

$$\frac{K_{cc} \times 0.242}{1.119 \times 10^{-7}} = -126 + 1.8 \left(\frac{0.2 \times 0.997 \times 9.193}{0.0102} \right) \left(\frac{0.0102}{0.997 \times 119 \times 10^{-7}} \right)$$

$$2162645.215 \cdot K_{cc} = -126 + 1.8 (13.41 \times 118.15)$$

$$K_{cc} = 1.26 \times 10^{-3} \text{ cm/sec}$$

over all mass transfer coefficient of circulating drops

$$\frac{1}{K_{oc}} = \frac{1}{9.6 \times 10^{-6}} + \frac{0.95}{1.26 \times 10^{-3}} = 104166.67 + 753.97$$

$$\frac{1}{K_{oc}} = 104920.64 = 9.53 \times 10^{-6}$$

$$K_{oc} = 9.53 \times 10^{-6} \text{ cm/sec}$$

$$\frac{K_{cc} \times 0.102}{1.119 \times 10^{-7}} = -126 + 1.8 \left(\frac{0.122 \times 0.497}{0.0102} \right) (10.36)^{0.5} \times 121.24$$

$$911528.15 K_{cc} = -126 + 108 (10.16 \times 121.24)$$

$$K_{cc} = 2.29 \times 10^{-3} \text{ cm/sec}$$

$$\frac{K_{cc} \times 0.109}{1.119 \times 10^{-7}} = -126 + 1.8 \left(\frac{0.104 \times 0.947 \times 10.45}{0.0102} \right)^{0.5} \times 121.24$$

$$929901.25 \cdot K_{cc} = -126 + 1.8 (10.31 \times 121.24) = 2123.97$$

$$K_{cc} = 2.28 \times 10^{-3} \text{ cm/sec}$$

$$\frac{K_{cc} \times 0.185}{1.119 \times 10^{-7}} = -126 + 1.8 \left(\frac{0.185 \times 0.947 \times 8.51}{0.0102} \right)^{0.5} \left(\frac{0.0102}{0.997 \times 1.119 \times 10^{-7}} \right)^{0.42}$$

$$1653261.89 K_{cc} = -126 + 1.8 (12.40 \times 121.24) \\ = 1.26 + 240.56 = 114.56$$

$$K_{cc} = 1.56 \times 10^{-3}$$

Oscillating drop regime

Dispersed phase mass transfer was firstly estimated by Rose and

Kintner equation

$$K_{do} = 0.45(D_d W)^{0.5}$$

$$W^2 = \frac{6b}{r^3} \left[\frac{n(n-1)(n+1)(n+2)}{(n+1)\rho_d + n\rho_c} \right]$$

$$n = 2$$

$$b = \frac{d_o^{0.225}}{1.242} = \frac{(0.222)^{0.225}}{1.242} = 0.574$$

$$r = \frac{0.222}{2} = 0.111 \text{ cm}$$

$$\delta = 35 \text{ dyne/cm}$$

$$W^2 = \frac{35 \times 0.5574}{(0.111)^3} \left[\frac{2(2.1)(2+1)(2+2)}{(2+1) \times 0.685 + 2 \times 0.947} \right]$$

$$14689.63 \left(\frac{2 \times 1 \times 3 \times 4}{3 \times 0.685 + 2 \times 0.947} \right)$$

$$14689.63 \left(\frac{30}{2.055 + 1.994} = \frac{34}{4.045} \right)^{5.42}$$

$$W = 295.14$$

$$K_{do} = 0.45(1.298 \times 10^{-7} \times 295.14)^{0.5} = 2.78 \times 10^{-3} \text{ cm/sec}$$

By ly Angelo

$$K_{do} = \sqrt{\frac{4D_{dw} \left[1 + E + \frac{3}{8} \right]}{n}}$$

$$E = 0.434 \left[\frac{W_{do}}{V_o} \right]^{-0.096} \left[\frac{d_o V_o^3 \rho_c}{\delta} \right]^{-0.53} + \left[\frac{M V_o}{\delta} \right]^{-0.11}$$

$$E = 0.434 \left[\frac{295.14 \times 0.222}{9.193} \right]^{-0.46} \left(0.222 \frac{(9.193)^3 \times 0.997}{35} \right)^{0.53}$$

$$- 0.53 \left[\frac{0.0102 \times 9.193}{35} \right]$$

$$0.434(0.405) \left(\frac{0.222(9.193)^3 \times 0.947}{35} \right)$$

$$0.434(0.406)(4.91) + 1.017$$

$$0.434 \times 0.406 \times 0.43 \times 1.912$$

$$0.145$$

$$E = 0.145$$

$$K_{do} = \sqrt{\frac{4D_o w \left(1 + i + \frac{3}{8} E^2 \right)}{\pi}}$$

$$= \sqrt{\frac{4 \times 1.298 \times 10^{-7} \times 295.14(1+0)45 + \frac{3}{8}(0.145)^2}{\pi}}$$

$$K_{do} = 7.49 \times 10^{-3} \text{ cm/sec. } \textit{Angleo}$$

The over all mass transfer coefficient

$$\frac{11}{K_o V_o} = \text{Oscillating drops}$$

$$K_{oo} = \frac{1}{K_{do}} + \frac{m}{K_{c.o}}$$

Continuos phase mass transfer coefficient

$K_{c.o}$ = was estimate by Garner correlation

$$\frac{K_{c.o} d_o}{D_c} = 50 + 0.0085 \text{ Re}_{sc}^{0.7}$$

$$\frac{K_{c.o} \times 0.222}{1.119 \times 10^{-7}} = 50 + 0.0085 \left(\frac{0.222 \times 9.193 \times 0.977}{0.0102} \right) \times \left(\frac{0.0102}{0.977 \times 1.119 \times 10^{-7}} \right)^{0.7}$$

$$1983914.21 K_{co}$$

$$= 50 + 0.0085 (199.48 \times 2969.97)$$

$$1983914.21 K_{co} \quad 76.94$$

$$K_{co} = 2.56 \times 10^{-3} \text{ cm/sec}$$

$$\frac{1}{K_{o.o}} = \frac{1}{K_{d.o}} + \frac{0.95}{K_{co}}$$

$$\frac{1}{K_{o.o}} = \frac{0.95}{3.88 \times 10^{-5}} + \frac{1}{2.78 \times 10^{-3}}$$

$$\frac{1}{K_{o.o}} = 24484.54 + 359.71$$

$$K_{o.o} = 4.03 \times 10^{-5} \text{ cm/sec by Rose and Kitner by Anglo}$$

$$K_{o.o} = K_{d.o} \left[\frac{1}{1 + m \sqrt{\frac{Dd}{Dc}}} \right]$$

$$K_{o.o} = 7.44 \times 10^{-3} \left[\frac{1}{1 + 0.95 \sqrt{\frac{1.298 \times 10^{-7}}{1.119 \times 10^7}}} \right]$$

$$7.49 \times 10^{-3} \left[\frac{1}{1.954} \right] = 3.31 \times 10^{-3} \text{ cm/sec.}$$

Oscillating drop regime Dis phase K_{do} by Rose and Kintner

$$K_{do} = 0.45(D_o W)^{0.5}$$

$$W^2 = \frac{\delta b}{r^3} \left[\frac{n(n-1)(n+1)(n+2)}{(n+1)\rho_d + n\rho_c} \right]$$

$$n = 2$$

$$b = \frac{d_o^{0.225}}{1.242} = \frac{(0.240)^{0.225}}{1.242} = 0.589$$

$$r = \frac{d_o}{2} = \frac{0.240}{2} = 0.12$$

$$\delta = 35$$

$$W^2 = \frac{35 \times 0.589}{(0.12)^3} \left[\frac{2(2-1)(2+1)(2+2)}{(2+1)\rho_n + n\rho_c} \right]$$

$$11828.70 \frac{(2 \times 1 \times 3 \times 4)}{3 \times 0.685 + 2 \times 0.497}$$

$$\frac{24}{2.055 + 1.994} = \frac{24}{4.49} = 5.93$$

$$W = 264.85$$

$$\text{Run N2 } K_{do} = 0.45(1.298 \times 10^{-7} \times 269.85)^{0.5} = 3.93 \times 10^{-3} \text{ cm/sec}$$

$$\text{Run N3 } r = 0.212 \quad \text{b. } \frac{(0.21)^{0.225}}{1.242} = 0.568$$

$$W^2 = \frac{\delta b}{r^3} (5.93) = w = \frac{d_o}{2}$$

$$\frac{35 \times 9.568}{1 - (0.212)} \times 5.93 = 314.61$$

$$K_{do} = 0.45(D_{dw}) \times (0.48(1.298 \times 10^{-7} \times 314.61))^{0.5}$$

$$2.87 \times 10^{-3} \quad \text{cm/sec.}$$

$$K_{do} = 0.45(D_d W)^{0.5}$$

$$K_{do} = 0.45(1.298 \times 10^{-7} \times W)^{0.5}$$

$$W^2 = \frac{\delta b}{r^3} \times 5.93$$

$$b = \frac{d_0}{1.292} = \frac{(0.205)}{1.242} = 0.564$$

$$W = \frac{35 \times 0.564}{(0.1085)^2} \times 5.93 = 329.70$$

$$K_{do} = 0.45(1.298 \times 10^{-7} \times 329.7)^{0.5} = 2.94 \times 10^{-3} \text{ cm/sec}$$

$$K_{do} = 0.45(1.298 \times 10^{-7} W)^{0.5}$$

$$W^2 = \frac{\delta b}{r^3} \times 5.93$$

$$b = \frac{d_0^{0.225}}{1.242} = \frac{(0.200)^{0.225}}{1.242} = 0.561$$

$$W^2 = \frac{d_o}{2} = \frac{0.2}{2} = 0.1$$

$$W^2 = \frac{35 \times 0.561}{(0.1)^3} \times 5.93 = 19635$$

$$W = \sqrt{19635} = 140.12$$

$$K_{do} = 0.45(1.298 \times 190.12)^{0.5} = 1.92 \times 10^{-3} \text{ cm/sec.}$$

K_{do} by Angelo

$$K_{do} = \sqrt{4D_d W \frac{1 + e + \frac{3}{8}E}{\pi}}$$

$$E = 0.434 \left[\frac{Wd_o}{V_o} \right]^{-0.46} \left[\frac{d_o V_o \rho_c}{\delta} \right]^{-0.53} \left[\frac{MV_o}{\delta} \right]^{-0.53}$$

$$E = 0.934 \left[\frac{264.89 \times 0.24}{8.51} \right]^{-0.46} \left[\frac{0.29 \times 8.512 \times 0.997}{35} \right]$$

$$\left(\frac{0.0102 \times 8.51}{35} \right)^{-0.11}$$

$$= 0.434 \times 1.935 \times 4.515 \times 1.935 = 1.384$$

$$0.434 \times 0.397 \times 0.467 \times 1.93 = 0.155$$

$$K_{do} = \sqrt{\frac{4 \times 1.298 \times 10^{-7} \times 264.84 \left(1 + 0.155 + \frac{3}{8}(0.155) \right)^2}{\pi}}$$

$$7.1410^{-3} \text{ cm/sec.}$$

$$K_{do} = \sqrt{4.D_o W \left(\frac{1 + E + \frac{3}{8}E}{\pi} \right)}$$

$$E = 0.434 \left[\frac{Wd_o}{V_o} \right]^{-0.46} \times \left[\frac{d_o V_o^3 \rho_c}{\delta} \right]^{-0.53} \times \left[\frac{MV_o}{\delta} \right]^{-0.11}$$

$$E = 0.434 \left[\frac{314.61 \times 0.212}{9.62} \right]^{-0.46} \times \left[\frac{0.212 \times (9.62)^3 \times 0.997}{35} \right]^{-0.53}$$

$$\left(\frac{0.0102 \times 9.62}{35} \right)^{-0.4}$$

$$E = 0.434 (0.413 \times 0.41 \times 1.908) = 0.140$$

$$K_{do} = \sqrt{\frac{4 \times 1.298 \times 10^{-7} \times 314.61 \left(1 + 0.14 + \frac{3}{8}(0.14)^2\right)}{\pi}}$$

$$K_{do} = 7.72 \times 10^{-3} \text{ cm/sec.}$$

$$K_{do} = 0.434(0.628 \times 0.386 \times 1.897) = 0.199$$

$$K_{do} = \sqrt{\frac{4 \times 1.298 \times 10^{-7} \times 140.12 \left(1 + 0.199 + \frac{3}{8}(0.199)^2\right)}{\pi}}$$

$$5.30 \times 10^{-8} \text{ cm/sec.}$$

$$K_{do} = 0.434 \left[\frac{347.99 \times 0.197}{10.36} \right]^{-0.46} \times \left[\frac{0.197 \times (10.36)^3 \times 0.997}{35} \right]^{-0.53} \left(\frac{0.0102 \times 10.36}{35} \right)^{-0.4}$$

$$K_{do} = 0.434 (0.4191037 \times 1.893) = 0.130$$

$$K_{do} = \sqrt{\frac{4 \times 1.298 \times 10^{-7} \times 347.12 \left(1 + 0.199 + \frac{3}{8}(0.13)^2\right)}{\pi}}$$

$$K_{do} = 8.07 \times 10^{-3} \text{ cm/sec.}$$

b) Continuous phase mass transfer coefficient was estimated by Garner et al correlation

$$\frac{K_{co} d_o}{D_c} = 50 + 0.0085 \text{ Re } s c^{0.7}$$

$$\frac{K_{co} \times 0.24}{1.119 \times 10^{-7}} = 50 + 0.0085 \left(\frac{0.24 \times 8.51 \times 0.997}{0.0102} \right) \left(\frac{0.0102}{0.977 \times 1.119 \times 10^{-7}} \right)^{0.7}$$

$$2149772.11 K_{co} = 50 + 0.0085(199.63 \times 2969.97)$$

$$K_{co} 2.37 \times 10^{-3} \text{ cm/sec.}$$

$$\frac{K_o K_{co}}{1.119} = 50 + 0.8085 \left(\frac{0.212 \times 9.6 \times 0.797}{0.0102} \right) \left(\frac{0.0102}{0.997 \times 1.119 \times 10^7} \right)^{0.7}$$

$$1894598.7 K_{co} = 50 + 0.0085(199.14 \times 2969.97)$$

$$K_{co} = 2.68 \times 10^{-3} \text{ cm/sec.}$$

$$\frac{0.205}{1.119 \times 10^{-7}} K_{co} = 50 + 0.0088 \left(\frac{0.205 \times 9.94 \times 0.997}{0.0102} \right) \left(\frac{0.0102}{0.977 \times 1.119 \times 10^{-7}} \right)$$

$$1831992.85 = 50 + 0.0085(199.18 \times 2964.97)$$

$$K_{co} = 2.77 \times 10^{-3} \text{ cm/sec.}$$

$$K_{co} = \frac{0.197}{1.119 \times 10^{-7}}$$

$$1760500.45 K_{co} = 50 + 0.0085 \left(\frac{0.197 \times 10.36 \times 0.997}{0.0102} \right) \times 2964.97$$

$$50 + 0.0085 \times 1.99.49 \times 2969.97$$

$$K_{co} = 2.89 \times 10^{-3} \text{ cm/sec.}$$

c) The over all mass transfer coefficient oscillating drops

$$\frac{1}{K_{oo}} = \frac{1}{K_{do}} + \frac{m}{K_{co}}$$

$$\frac{1}{K_{oo}} = \frac{1}{714 \times 10^{-7}} + \frac{0.95}{2.37 \times 10^{-3}} = 1900560.22 + 2.4927 \times 10^{-3}$$

$$K_{o.o} = 7.14 \times 10^{-7} \text{ cm/sec.}$$

$$\frac{1}{K_{oo}} = \frac{1}{7.72 \times 10^{-3}} + \frac{0.95}{2.65 \times 10^{-3}} = 129.536 + 2.07 \times 10^{-3} \text{ cm/sec.}$$

$K_{o.o}$ by Angelo

$$K_{o.o} = K_{do} \left[\frac{1}{1 + m \sqrt{\frac{Dd}{Dc}}} \right]$$

$$K_{o.o} = 7.14 \times 10^{-3} \left[\frac{1}{1 + 0.95 \frac{1}{\sqrt{\frac{1.298 \times 10^{-7}}{1.119 \times 10^{-7}}}}} \right] = 3.53 \times 10^{-3}$$

The theoretical over mass transfer coefficient for the whole drop population by Rose and Kintner and Garner

$$K_{cal} = K_{oc}V + K_{o,o}(1-V)$$

$$K_{cal} = 9.53 \times 10^{-6} \times 0.3 + 4.03 \times 10^{-5} \times 0.7 = 3.11 \times 10^{-5} \text{ cm/sec.}$$

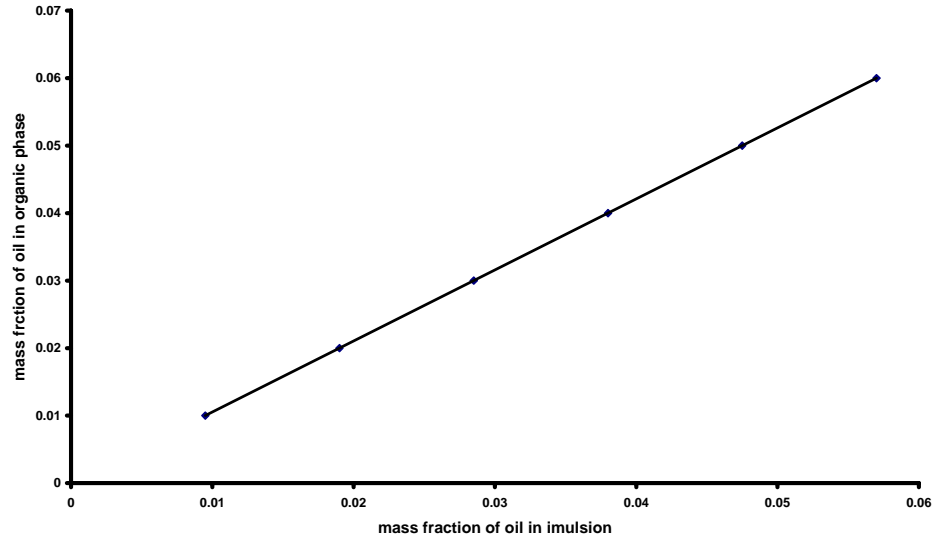
Chemical and physical properties of n.hexane

density	0.658 g/cm ³
Molecular weight	86
Boiling point	68o c
Freezing point	- 95o c
Flash point	-22o c
Viscosity	0.294 cps
Surface tension	18.48 dyn/cm

Chemical and physical properties of Emulsion

1. Density 0.977g\ cm³
2. Viscosity 0.324 cps

equilibrium relationship



equilibrium relationship

